Neurotherapeutics 21 (2024) e00357

Contents lists available at ScienceDirect

Neurotherapeutics

journal homepage: www.sciencedirect.com/journal/neurotherapeutics

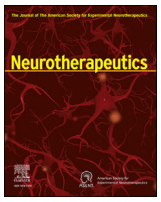

Original Article

A phosphodiesterase 4 (PDE4) inhibitor, amlexanox, reduces neuroinflammation and neuronal death after pilocarpine-induced seizure

Hyun Wook Yang [a], A Ra Kho [b,c], Song Hee Lee [a], Beom Seok Kang [a], Min Kyu Park [a], Chang Jun Lee [a], Se Wan Park [a], Seo Young Woo [a], Dong Yeon Kim [a], Hyun Ho Jung [a], Bo Young Choi [d,e], Won Il Yang [e,f], Hong Ki Song [g,i], Hui Chul Choi [h,i], Jin Kyu Park [a,1,*], Sang Won Suh [a,i,1,*]

[a] Department of Physiology, Neurology, Hallym University, College of Medicine, 1-Okcheon Dong, 39 Hallymdaehak-gil, Chuncheon 200-708, Republic of Korea
[b] Neuroregeneration and Stem Cell Programs, Institute for Cell Engineering, Johns Hopkins University School of Medicine, Baltimore, MD 21205, USA
[c] Department of Neurology, Johns Hopkins University School of Medicine, Baltimore, MD 21205, USA
[d] Department of Physical Education, Hallym University, Chuncheon 24252, Republic of Korea
[e] Institute of Sport Science, Hallym University, Chuncheon 24252, Republic of Korea
[f] Department of Sport Industry Studies, Yonsei University, Seoul 03722, Republic of Korea
[g] Neurology, Kangdong Sacred Heart Hospital, Seoul 05355, Republic of Korea
[h] Neurology, Hallym University Chuncheon Sacred Heart Hospital, Chuncheon 24253, Republic of Korea
[i] Hallym Institute of Epilepsy Research, Hallym University, Chuncheon 24252, Republic of Korea

ARTICLE INFO

Keywords:
Epilepsy
cAMP
Phosphodiesterase4
Lysosome
Autophagy
Neuro-inflammation

ABSTRACT

Epilepsy, a complex neurological disorder, is characterized by recurrent seizures caused by aberrant electrical activity in the brain. Central to this study is the role of lysosomal dysfunction in epilepsy, which can lead to the accumulation of toxic substrates and impaired autophagy in neurons. Our focus is on phosphodiesterase-4 (PDE4), an enzyme that plays a crucial role in regulating intracellular cyclic adenosine monophosphate (cAMP) levels by converting it into adenosine monophosphate (AMP). In pathological states, including epilepsy, increased PDE4 activity contributes to a decrease in cAMP levels, which may exacerbate neuroinflammatory responses. We hypothesized that amlexanox, an anti-inflammatory drug and non-selective PDE4 inhibitor, could offer neuroprotection by addressing lysosomal dysfunction and mitigating neuroinflammation, ultimately preventing neuronal death in epileptic conditions. Our research utilized a pilocarpine-induced epilepsy animal model to investigate amlexanox's potential benefits. Administered intraperitoneally at a dose of 100 mg/kg daily following the onset of a seizure, we monitored its effects on lysosomal function, inflammation, neuronal death, and cognitive performance in the brain. Tissue samples from various brain regions were collected at predetermined intervals for a comprehensive analysis. The study's results were significant. Amlexanox effectively improved lysosomal function, which we attribute to the modulation of zinc's influx into the lysosomes, subsequently enhancing autophagic processes and decreasing the release of inflammatory factors. Notably, this led to the attenuation of neuronal death in the hippocampal region. Additionally, cognitive function, assessed through the modified neurological severity score (mNSS) and the Barnes maze test, showed substantial improvements after treatment with amlexanox. These promising outcomes indicate that amlexanox has potential as a therapeutic agent in the treatment of epilepsy and related brain disorders. Its ability to combat lysosomal dysfunction and neuroinflammation positions it as a potential neuroprotective intervention. While these findings are encouraging, further research and clinical trials are essential to fully explore and validate the therapeutic efficacy of amlexanox in epilepsy management.

* Corresponding authors.
E-mail addresses: akqjqtj5@hallym.ac.kr (H.W. Yang), akho3@jhu.edu (A.R. Kho), sshlee@hallym.ac.kr (S.H. Lee), bskang@hallym.ac.kr (B.S. Kang), D22029@hallym.ac.kr (M.K. Park), doog0716@hallym.ac.kr (C.J. Lee), M2022087@hallym.ac.kr (S.W. Park), M22091@hallym.ac.kr (S.Y. Woo), M22525@hallym.ac.kr (D.Y. Kim), wjdgusgh1021@hallym.ac.kr (H.H. Jung), bychoi@hallym.ac.kr (B.Y. Choi), wonil4u@hallym.ac.kr (W.I. Yang), hksong0@hallym.oc.kr (H.K. Song), dohchi@hallym.ac.kr (H.C. Choi), jinkyupark71@hallym.ac.kr (J.K. Park), swsuh@hallym.ac.kr (S.W. Suh).
[1] Equally contributed.

https://doi.org/10.1016/j.neurot.2024.e00357
Received 31 October 2023; Received in revised form 8 April 2024; Accepted 8 April 2024

Abbreviations

PDE4	Phosphodiesterase-4
ATP	Adenosine triphosphate
G-PCRs	G Protein Coupled Receptors
AC	Adenylyl Cyclase
cAMP	cyclic Adenosine monophosphate
PKA	Protein Kinase A
AMP or 5′-AMP	Adenosine monophosphate
$GABA_A$ receptors	γ-Aminobutyric acid type A receptors
AEDs	Anti Epileptic Drugs
TBI	Traumatic Brain Injury
IL-6	interleukin-6
TNF-α	Tumor necrosis factor – α
COX-2	Cyclooxygenase-2
BBB	Blood Brain Barrier
pH	potential of hydrogen
IKKε	nuclear factor kappa-B kinase subunit epsilon
TBK1	Tank Binding Kinase1
NAFLD	non-alcoholic fatty liver disease
ROS	Reactive oxygen species
CA1, CA3	Cornu Ammonis1, Cornu Ammonis3
DG	Dentate Gyrus
NIH	National Institute of Health
SD-rats	Sprague-Dawley rats
ARRIVE	Animal Research: Reporting in Vivo Experiments
LAMP2	Lysosome-Associated Membrane Protein 2
LC3B	Light Chain 3 B
NeuN	Neuronal nuclear protein
GFAP	Glial fibrillary acidic protein
Iba-1	Ionized calcium-binding adapter molecule 1
C3	Complement 3
CD68	Cluster of Differentiation 8
MAP2	Microtubule Associated Protein 2
4HNE	4-hydroxyl-2-nonenal
DAPI	4′,6-diamidino-2-phenylindole
ABC	Avidin Biotin Complex
DAB	3,30-diaminobenzidine
PBS	Phosphate Buffered Saline
D.W	Distilled Water
SDS-PAGE	sodium dodecyl sulfate–polyacrylamide gel electrophoresis
TBS-T	Tris-buffered saline with Tween
RIPA Buffer	Radio-Immunoprecipitation Assay Buffer
PVDF	polyvinylidene difluoride
mNSS	Modified neurological severity score

Introduction

Epilepsy is a chronic neurological disorder characterized by recurrent unprovoked seizures [1]. Epilepsy manifests in different forms, with over 60% of cases being focal epilepsy primarily affecting the temporal lobe [2]. The precise mechanism of seizures in epilepsy is still unknown, and ongoing research aims to unravel it. Furthermore, each individual's experience with epilepsy requires a unique approach due to its variability [3]. Previously recognized mechanisms of epilepsy included a decline in inhibitory neurotransmitters and diminished sensitivity of γ-Aminobutyric acid type A ($GABA_A$) receptors [4,5]. Another mechanism involves the activation of specific receptors, leading to seizures in a rat model. This activation results in an influx of intracellular Ca2+, triggering the seizure activity [6,7]. Epilepsy can be caused by various acquired factors, including tumors, infections, traumatic brain injuries (TBI), and other underlying conditions [8]. Severe epilepsy can give rise to cognitive and memory impairments due to neuronal death in the hippocampus, potentially leading to more significant neurological complications [9]. The current approaches for treating seizures involve medication and surgical interventions. However, there are cases where certain patients do not respond to anti-epileptic drugs (AEDs) despite being on medication [10]. Identifying suitable candidates for effective epilepsy treatments is crucial and remains a significant challenge to be addressed in the future.

Neuroinflammation refers to inflammation that occurs within the nervous system, which encompasses the brain and spinal cord [11]. Neuroinflammation in epilepsy is triggered by various inflammatory factors, which have the potential to worsen neurological conditions, including global cerebral ischemia and TBI [9,12,13]. In animal models of epilepsy, cytokines such as interleukin-6 (IL-6) and tumor necrosis factor- α (TNF-α) are elevated, along with increased levels of inflammatory factors like cyclooxygenase-2 (COX-2) [14–16]. This inflammation caused by these factors contributes to the development of epilepsy [16]. The upregulation of COX-2 is particularly significant as it plays a major role in disrupting the blood-brain barrier (BBB) [16]. Furthermore, neuroinflammatory conditions such as epilepsy can impair autophagy, a cellular process involved in the degradation and recycling of cellular components. Reduced autophagy function in these neurological diseases can result in excessive inflammation, leading to neuronal cell death [17].

Phosphodiesterase-4 (PDE4) is an enzyme responsible for the hydrolysis of cyclic adenosine monophosphate (cAMP) to adenosine monophosphate (AMP or 5′-AMP) [18]. Cyclic adenosine monophosphate (cAMP) functions as a second messenger, synthesized from adenosine triphosphate (ATP) by the enzyme adenylyl cyclase (AC) [19]. Activation of cAMP occurs through stimuli, including neurotransmitters, acting on G-protein coupled receptors (GPCRs). Additionally, cAMP regulates protein kinase A (PKA) and cAMP response element-binding protein (CREB) [20]. Overexpression of phosphodiesterase-4 (PDE4) has been implicated in the development of various neurological diseases, including stroke, Parkinson's disease (PD), and other related conditions [21–23]. Suppression of phosphodiesterase-4 (PDE4) leads to the accumulation of zinc within the lysosome. This accumulation results in a decrease in lysosomal potential of hydrogen (pH) and an enhancement of lysosomal function [24,25].

Amlexanox is an anti-inflammatory drug that functions as an inhibitor of nuclear factor kappa-B kinase subunit epsilon (IKKε)/TANK-binding kinase 1 (TBK1) [26]. Additionally, it is recognized as a non-selective inhibitor of phosphodiesterase 4B (PDE4B) [27] Recently, there has been research exploring the potential use of amlexanox as a treatment for conditions such as obesity, type 2 diabetes, and non-alcoholic fatty liver disease (NAFLD) [27–30]. However, currently there is limited or no scientific research investigating the use of amlexanox specifically for the treatment of neurological diseases like epilepsy. Its potential therapeutic applications in the field of neurology remain to be explored. This study aims to evaluate the efficacy of amlexanox as a therapeutic agent in pilocarpine-induced seizures. Additionally, it seeks to investigate whether amlexanox inhibits PDE4 activity and reduces neuroinflammatory factors by improving lysosome and autophagy functions.

Methods

Ethics statement and care of experiment animal

This study was approved by the Laboratory Animal Guides and Laboratory Rules published by the National Institute of Health (NIH), and this animal experiment was conducted according to the criteria of the Laboratory Animal Research Committee (protocol #Hallym 2022-22). The

animal used in this experiment is male Sprague–Dawley rats (SD-rats, 280–350 g, 8-weeks old, DBL Co, Korea). Laboratory animal is constant humidity (55 ± 5%) and room temperature (22 ± 2 °C) and lighting in the room is kept for a week for 12 h apart on and off is designed to (on at 6:00 and off at 18:00). The guidelines for this experiment were designed by ARRIVE (Animal Research: Reporting in Vivo Experiment).

Seizure induction

To induce seizures in the experimental animals, the following procedure was conducted. 19 h prior to the administration of pilocarpine, lithium chloride (127 mg/kg, i.p, Sigma-Aldrich Co., St. Louis, MO, USA) was injected intraperitoneally. 30 min before the administration of pilocarpine, scopolamine (2 mg/kg, i.p, Sigma-Aldrich Co., St. Louis, MO, USA) was injected intraperitoneally. After the 30-min interval following scopolamine administration, pilocarpine (25 mg/kg, i.p, Sigma-Aldrich Co., St. Louis, MO, USA) was injected intraperitoneally. The stages of seizure were assessed using the Racine scale, which consists of five stages: Stage 1: Mouth and facial movement. Stage 2: Head nodding. Stage 3: Forelimb clonus. Stage 4: Rearing with forelimb clonus. Stage 5: Rearing and falling with forelimb clonus. Diazepam (10 mg/kg, French, France Neuilly Sur Valium, Hoffman, Seine La Roche) was administered 1 h after the onset of seizures. If recurrent seizures persisted, additional doses of diazepam were injected. This protocol was designed to induce seizures in the animals and evaluate their seizure behavior according to the Racine scale. Diazepam was used as an anticonvulsant to terminate prolonged or recurrent seizures.

Experimental design and drug administration

In the experiment, the animals were divided into four groups: 1) Sham Vehicle: This group served as the control group without seizures or amlexanox treatment. They received vehicle injections (placebo) instead. 2) Sham Amlexanox: This group received sham treatment without seizures, but they were administered amlexanox (100 mg/kg, i.p, Arctom, Westlake Village, CA, USA) once a day for 7 days. 3) Seizure Vehicle: This group experienced pilocarpine-induced seizures but received vehicle injections (placebo) instead of amlexanox. 4) Seizure Amlexanox: This group experienced pilocarpine-induced seizures and received amlexanox (100 mg/kg, i.p, Arctom, Westlake Village, CA, USA) once a day for 7 days after the seizures. The amlexanox injections were administered intraperitoneally (i.p) at a dose of 100 mg/kg. The treatment duration was 7 days starting from the day of seizure induction. A week after the seizures, the animals were sacrificed to obtain brain tissue for histological evaluation. This histological evaluation aimed to examine the effects of amlexanox treatment on various parameters related to seizures, as described in our previous statements.

Assessing drug side effects

To evaluate the side effects of the drug, both acute and chronic phases in the seizure model were analyzed. During the acute phase, which spans one week, we monitored weight changes following the administration of amlexanox across different groups. This involved daily weight recordings from the onset of induced seizures and the commencement of drug treatment, continuing for one week. The resulting data were plotted in a graph. For the chronic phase, lasting four weeks, we tracked weight fluctuations and calculated mortality rates. This extended over a four-week period, with the mortality rate represented as a percentage, reflecting the proportion of deceased animals relative to the total number in the study over these four weeks.

Brain sample preparation

To sacrifice the animals and prepare the brain tissue for further analysis, the following procedure was performed. The seizure-experienced animals were anesthetized using urethane (1.5 g/kg, i.p). After anesthesia, 0.9% saline and 4% paraformaldehyde were administered into the heart to perfuse the animal and fix the tissues. The brain was quickly and accurately removed from the skull following perfusion. The harvested brains were post-fixed with 4% paraformaldehyde for 1 h to enhance tissue preservation. After post-fixation, the brains were transferred to a 30% sucrose solution and kept there until they sank to the bottom. This step helps to protect the tissue and facilitate cryosectioning. Two days later, the brains were sectioned into slices with a thickness of 30 μm using a cryostat microtome (CM1850; Leica, Wetzlar, Germany). These sections are thin enough for subsequent histological analysis. The brain sections were collected and stored in a 2 ml tube containing a suitable storing solution to preserve their integrity and prevent degradation. Following this procedure, we ensured that the brain tissue obtained from the seizure-experienced animals was adequately fixed, preserved, and prepared for further histological evaluations and analysis.

Detection of live neuron

To identify living neurons after pilocarpine-induced seizure, the following steps were performed for neuronal nuclei (NeuN) staining. The brain tissue sections were pretreated to remove any remaining blood cells from the tissue. The brain tissue sections were stored overnight in mouse anti- Neuronal nuclear protein (NeuN) antibodies (diluted 1:500, Millipore, Bilica, MA, USA) in a phosphate buffered saline (PBS) solution containing 0.3% Triton X-100. This step allows the antibodies to bind specifically to NeuN, a marker for neurons. After washing the tissue, anti-mouse IgG (diluted 1:250, Burlingame, Vector, CA, USA) was applied to the tissue and allowed to stain at room temperature for 2 h. The secondary antibody binds to the primary antibody, enhancing the visualization of NeuN-positive neurons. The tissue was treated with an avidin-biotin complex (ABC) composite solution at room temperature for 2 h. The ABC complex amplifies the signal from the primary and secondary antibodies, further increasing the detection of NeuN-positive neurons. 3,30-diaminobenzidine (DAB ager, Sigma-Aldrich Co., St. Louis, MO, USA) was applied to the tissue for 1 min and 30 s. DAB reacts with the ABC complex to produce a brown color, indicating the presence of NeuN-positive neurons. The stained tissue sections were placed on slides, allowed to dry, and mounted with Canada balsam. This step preserves the stained tissue and allows for further analysis and observation under a microscope. By performing these steps, We were able to stain the brain tissue sections for NeuN, identifying and visualizing living neurons in the context of pilocarpine-induced seizure.

Immunofluorescence analysis

To perform immunohistochemistry and confirm the therapeutic effect of amlexanox after seizure, the following steps were conducted using brain tissue collected at 12 h and 7 days after the seizure. The cut tissue was washed three times for 10 min with 0.01 M PBS (phosphate-buffered saline) to remove any debris or contaminants. A pretreatment solution consisting of 90% methanol, distilled water (D.W), and 30% hydrogen peroxide (30% H_2O_2) was applied to the tissue for 15 min to remove any blood present in the tissue. The tissue was immersed in a PBS antibody solution containing 0.3% Triton X-100 and incubated overnight at 4 °C. Primary antibodies were used as follows: mouse anti-4-hydroxyl-2-nonenal. (4HNE, diluted 1:500; Alpha Diagnostic Intl. Inc., San Antonio, TX, USA), rabbit anti- Microtubule Associated Protein 2 (MAP2, diluted 1:200; Abcam, Cambridge, UK), goat anti-Iba1 (diluted 1:500; Abcam, Cambridge, UK), mouse anti- Cluster of Differentiation 68(CD68, diluted 1:100; Bio-Rad, Hercules, CA, USA), rabbit anti- Glial fibrillary acidic protein (GFAP, diluted 1:1000; Abcam, Cambridge, UK), goat anti-Complement 3(C3, diluted 1:300; Invitrogen, Grand Island, NY, USA), rabbit anti-phosphodiesterase4B(PDE4B, diluted 1:250, FabGennix, Frisco, USA), rabbit anti-tumor necrosis factor- α (TNF-α, diluted 1:250, Abcam, Cambridge, UK), and mouse anti-interleukin-6(IL-6, diluted

1:500, Abcam, Cambridge, UK). The tissue was washed three times in 0.01 M PBS for 10 min each to remove any excess primary antibodies. The tissue was immersed in a secondary antibody solution (Alexa Fluor 488 or 594 donkey anti-rabbit, mouse, goat IgG) diluted 1:250 in PBS containing 0.3% Triton X-100. This incubation was performed at room temperature for 2 h. The tissue was also stained with DAPI (4,6-diamidino-2-phenylindole) diluted 1:1000 in PBS. DAPI is a fluorescent dye that stains DNA, allowing for visualization of cell nuclei. Finally, the tissue was placed on a slide glass and mounted with a DPX solution (Sigma-Aldrich), which is a mounting medium used to preserve the stained tissue. These steps allowed for the immunohistochemical staining of specific markers, including 4HNE, MAP2, Iba1, CD68, GFAP, C3, PDE4B, IL-6, and tumor necrosis factor-α (TNF-α) to examine various aspects of neuronal and glial activity and identify the therapeutic effects of amlexanox after seizure. We observed the brain sections with a fluorescence microscope (Model: BX53T-32X01/FL and DP74-ST, Olympus, Tokyo, Japan).

Detection of blood brain barrier disruption

After washing the cut tissue three times for 10 min with 0.01 M PBS, a 15-min treatment was performed to remove blood from the tissue. The tissue was then immersed in a PBS antibody solution containing 0.3% Triton X-100 and anti-rat IgG (diluted 1:250, Burlingame, Vector, CA, USA) for 2 h at room temperature. Following this, the tissue was washed three times in 0.01 M PBS for 10 min each. Next, the tissue was immersed in an ABC complex solution at room temperature for 2 h. The ABC complex is commonly used in immunohistochemistry to enhance the detection of antigens. After the incubation with the ABC complex, the tissue was treated with DAB ager (Sigma-Aldrich Co., St. Louis, MO, USA) for 1 min and 30 s. DAB is a chromogen that produces a brown precipitate when reacted with peroxidase, allowing for visualization of the antigen of interest. The tissue was then placed on a slide, dried, and mounted with Canada balsam, which is a mounting medium commonly used in histology to preserve the stained tissue and provide a clear optical path for microscopic examination.

Detection of zinc accumulation and lysosome

To perform FluoZin-3 and Lysotracker staining, fresh frozen brain tissue was obtained from deeply anesthetized animals using 1–1.5% isoflurane and an oxygen/nitrogen oxide mixture (25:75) from David Kopf Instruments (Tujunga, CA, USA). The brain tissue was harvested without perfusion and rapidly frozen using powdered dry ice. It was then stored in a deep freezer until further use. For sectioning, the frozen brain tissue was cut into 10 μm thick sections using a cryostat. The cut tissue sections were mounted on coated slides and allowed to air-dry for 1 h. To create a hydrophobic barrier around the tissue and ensure precise application of staining solutions, ImmEdge™ Pen (Vector Laboratories, Burlingame, CA, USA) was used. The tissue sections were fixed in 4% paraformaldehyde for 30 min. After 30 min, the tissue was washed three times for 1 min each with 0.01 M PBS. The tissue was then immersed in a PBS antibody solution containing 0.3% Triton X-100, 1 μM FluoZin™-3 (Invitrogen, Grand Island, NY, USA), and 5 μM LysoTracker™ Red DND-99 (Invitrogen, Grand Island, NY, USA). This solution helps in staining intracellular zinc ions with FluoZin-3 and acidic compartments (such as lysosomes) with LysoTracker™ Red DND-99. The tissue was incubated in this solution for 45 min. After 45 min, the tissue was washed three times for 1 min each with 1x PBS to remove any unbound staining reagents. Finally, the tissue was placed on a slide glass and mounted with a DPX solution (Sigma-Aldrich), which is a mounting medium used to preserve the stained tissue. By following above methods, the FluoZin-3 and Lysotracker staining allows for the visualization and quantification of intracellular zinc ions and lysosomes, respectively, in the brain tissue sections. We observed the brain sections with a fluorescence microscope (Model: LSM710, Carl Zeiss, Oberkochen, Germany).

Western blot

Hippocampal tissue used for Western blot analysis was perfused with cold saline. The tissue was then homogenized in a lysis buffer containing radio-immunoprecipitation assay (RIPA) buffer, protease inhibitor, and phosphatase inhibitor. After incubating the tissue on ice for 30 min, it was centrifuged at 14,000 rpm, 4 °C for 20 min. The supernatant was collected, and protein quantification was performed using Bradford protein analysis. The quantified protein samples were prepared at a concentration of 25 μg and loaded onto sodium dodecyl sulfate–polyacrylamide gel electrophoresis (SDS-PAGE) gels. The gels had different compositions, ranging from 8% to 15%, depending on the target protein. The proteins were separated by electrophoresis and then transferred onto a polyvinylidene difluoride (PVDF) membrane. To minimize non-specific staining, the membrane was blocked with either 5% skim milk or 5% BSA at room temperature. After blocking, the membrane was incubated overnight at 4 °C with primary antibodies, including lysosome-associated membrane protein 2 (LAMP2), light chain 3 B (LC3B), cyclooxygenase-2 (COX-2), and β-actin. These antibodies were diluted according to the manufacturer's instructions. The following day, the membrane was washed three times with Tris-buffered saline with Tween (TBS-T) and incubated at room temperature for 1 h with secondary antibodies (anti-rabbit IgG and anti-mouse IgG) diluted 1:5000. After three additional washes with TBS-T, protein bands on the membrane were visualized using a chemiluminescence imaging system device such as the Amersham imager 680 machine from GE Healthcare.

Behavior tests

Modified neurological severity score (mNSS)

After the seizures, a modified neurological severity score (mNSS) test was conducted to assess the animals' motor function, seizure frequency, and latency. The scores ranged from 0 (no impairment) to 18 (severe impairment) and were evaluated daily from 4 h to 14 days after the seizure. The mNSS includes five categories: tail flexion (3 points), floor walking (3 points), responses to visual and tactile stimuli and limb muscle condition (2 points), balance on a beam (6 points), and reflex absence along with seizure activity (4 points). Additionally, the seizure frequency and latency were specifically evaluated under the 'seizure activity' criterion, with scores of 0 or 1 given.

Barnes maze test

To assess post-seizure spatial cognitive recovery, we conducted a Barnes maze test on the rats treated with amlexanox. The rats that had been epileptic for two weeks were split into two groups: one received immediate amlexanox treatment after the seizure, while the other had a rest period before treatment. The Barnes maze consisted of a circular board (122 cm diameter) with multiple holes, with only one leading to an escape cage (7 cm hole diameter). Each rat's ability to locate the escape hole was timed over 14 days, with a maximum of 2 min per trial. After two weeks, the rats were euthanized for sample analysis.

Data analysis

All data were presented as mean ± standard error of the mean (S.E.M). *P*-values were considered statistically significant below 0.05. Comparisons between the seizure vehicle group and the amlexanox group were performed by Mann-Whitney *U* test. Comparisons between the other four groups were analyzed by Kruskal-Wallis test followed by Bonferroni post hoc test.

Results

Study of amlexanox's impact on seizure frequency, body weight, and mortality rate following pilocarpine-induced seizures

Amlexanox was administered at a dose of 100 mg/kg daily following the pilocarpine-induced seizures. The animals were euthanized at various intervals (12 h, 72 h, 7 days, and 1 month after a seizure) for brain histological analysis (refer to Fig. 1A). Their seizure behaviors were evaluated using Racine's scale, noting seizure onset at around 30 min following pilocarpine administration (see Fig. 1B), confirming the effectiveness of the seizure model. We monitored the body weight changes to evaluate amlexanox's potential side effects. Interestingly, there was a significant difference in the body weight changes between the amlexanox-treated and control groups (Fig. 1C), suggesting that amlexanox had a minimal impact on the body weight during the study. The mortality rate was another critical measure. In the control group (seizure vehicle group), the mortality rate was as high as 92% during the trial, while it was reduced to 50% in the amlexanox-treated group (Fig. 1D). Initially, 14 rats were included in each group, with an additional 10 rats introduced in the control group due to the high mortality rates. This underscores the severity of pilocarpine-induced seizures (Fig. 1E). Furthermore, we evaluated the seizure frequency and latency using the mNSS test following the seizure. Notable differences were observed between the control and amlexanox groups on days 4, 5, and 7–14 (Fig. 1F).

In conclusion, our findings indicate that amlexanox treatment did not significantly affect the animals' body weight. However, it showed potential neuroprotective benefits by reducing seizure frequency and mortality. This was evident in the histological evaluation of the brain tissue, particularly for chronic seizures, suggesting its efficacy in both acute and chronic seizure conditions without notable side effects.

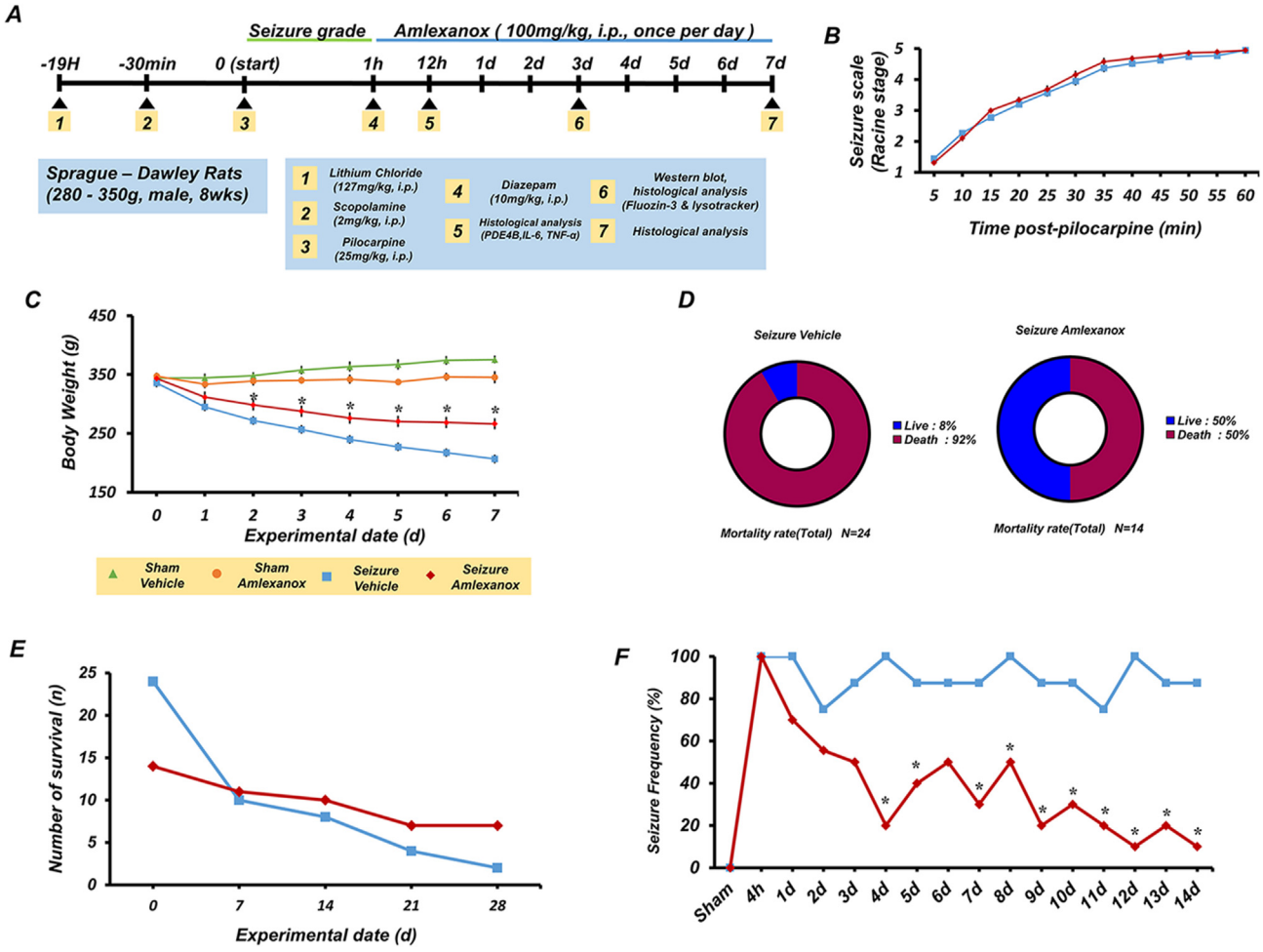

Fig. 1. Study of Amlexanox's Impact on Seizure Frequency, Body Weight, and Mortality Rate in Pilocarpine-Induced Seizures. A. Experimental Timeline: Outlines the procedure involving pilocarpine administration and the subsequent monitoring of the seizure intensity at 5-min intervals until Stage 4 (rearing with forelimb clonus). Additionally, details the schedule for body weight measurements in the various groups (sham vehicle, sham amlexanox, seizure vehicle, and seizure amlexanox) following the seizure episodes. B. Seizure Assessment: Illustrates the frequency of the seizure evaluation, conducted every 5 min following pilocarpine administration, until Stage 4 was reached. Presents the duration taken by each group to reach Stage 4, highlighting that the average onset time for seizures in both the seizure vehicle and seizure amlexanox groups was around 30 min. C. Body Weight Comparison: Shows body weight data for each group (sham vehicle, sham amlexanox, seizure vehicle, seizure amlexanox) gathered after the occurrence of seizures. D. Mortality Rate Pie Chart: Displays the mortality rates in rats subjected to pilocarpine-induced seizures, with the blue segment representing survival and the purple segment indicating mortality. E. Survival Graph: Plots the weekly survival counts of the experimental animals in the model, categorized by week. F. Seizure Frequency Graph: Depicts the frequency of seizures observed in the model during the mNSS test, spanning from 4 h after induction to 14 days. The graph presents the mean frequency of seizures, noting a statistically significant difference ($p < 0.05$) between the vehicle group and the amlexanox-treated group (ANOVA after repeated-measures testing, seizure frequency: time: $F = 2.877$, $p = 0.001$; group: $F = 30.202$, $p < 0.001$; interaction: $F = 2.179$, $p = 0.009$).

Amlexanox's effect on PDE4B expression, pro-inflammatory factors, and zinc levels in lysosomes following seizures

This study investigated the impact of amlexanox on phosphodiesterase-4B (PDE4B) expression following pilocarpine-induced seizures. We examined the PDE4B levels in the hippocampi of rats at 12 h following a seizure. The results showed a significant increase in PDE4B expression after the seizure, indicating that elevated PDE4B activity may contribute to initial neuronal damage. However, when amlexanox was administered post-seizure, it significantly suppressed PDE4B activity. The amlexanox-treated group exhibited a remarkable 68.5% reduction in PDE4B activity compared to the seizure-vehicle group (Fig. 2A and B). These findings suggest that amlexanox effectively inhibits PDE4B activity in the hippocampus following seizures, potentially contributing to its neuroprotective effects. This reduction was as follows: sham vehicle = 2.84 ± 0.44, sham amlexanox = 3.02 ± 0.25, seizure vehicle = 13.13 ± 1.55, seizure amlexanox = 4.13 ± 0.33.

Furthermore, Furthermore, we analyzed the effects of amlexanox on the zinc levels within the endoplasmic reticulum and on lysosome activation. Using FluoZin-3 and LysoTracker staining, we evaluated the quantity of intra-endoplasmic reticulum zinc and acidic lysosomes 72 h after the seizure. An increase in zinc in the intra-endoplasmic reticulum was noted in the seizure group, suggesting a homeostatic response to neurodegenerative conditions. Post-seizure treatment with amlexanox led to a further 69.8% increase in zinc levels, indicating enhanced lysosome activation and autophagy due to increased PDE4B activity (Fig. 2CandD). The specific rate of increase was as follows: seizure vehicle = 15.95 ± 4.53, seizure amlexanox = 52.76 ± 4.99.

We also assessed the anti-inflammatory effects of amlexanox by measuring the levels of tumor necrosis factor (TNF-α) and interleukin-6 (IL-6) at 12 h following the seizure. The results demonstrated an increase in pro-inflammatory factors after the seizure, suggesting that this may lead to an increase in neuronal death. However, administering amlexanox 12 h after the seizure reduced pro-inflammatory markers (Fig. 2E–G). Specifically, the detailed results showed that IL-6 increased by 86% compared to the sham group, but amlexanox administration group decreased it by 60.9% compared to the seizure vehicle group. Similarly, TNF-α increased by 96% compared to the sham group, but the amlexanox administration group decreased it by 61.7% compared to the seizure vehicle group. Therefore, further analysis and investigation are necessary to understand the specific mechanisms by which PDE4B modulation influences neuronal damage and the overall therapeutic implications of targeting PDE4B in seizure treatment. The specific decreases were as follows: for TNF-α, sham vehicle = 1.27 ± 0.08, sham amlexanox = 1.13 ± 0.14, seizure vehicle = 31.91 ± 2.88, seizure amlexanox = 12.2 ± 0.82; for IL-6, sham vehicle = 6.51 ± 0.09, sham amlexanox = 6.94 ± 0.88, seizure vehicle = 46.62 ± 2.81, seizure amlexanox = 18.21 ± 2.32.

These findings highlight the need for further research to elucidate how PDE4B modulation affects neuronal damage and the potential therapeutic implications of targeting PDE4B in seizure treatment.

Amlexanox enhances autophagy and lysosomal function while reducing neuroinflammation

We conducted a study to evaluate the protein levels of lysosomal function, autophagy, and inflammatory factors, specifically cyclooxygenase-2 (COX-2), following seizures. Protein levels of lysosome-associated membrane protein 2 (LAMP2), light chain3B (LC3B), and COX-2 were measured 72 h after the seizure event.

To assess lysosomal function and autophagy levels, we examined the protein levels of LAMP2 and LC3B after the seizures. Our findings revealed a significant reduction in LAMP2 and LC3B levels compared to the sham group, indicating a decline in lysosomal function and autophagy following seizures. However, the group treated with amlexanox demonstrated an improvement in lysosomal function and autophagy compared to the seizure vehicle group (Fig. 3A–C). Specifically, LAMP2 levels increased by 37.7% compared to the seizure vehicle group, while LC3B levels increased by 43.5%. These results suggest that amlexanox administration enhances lysosomal function and autophagy. The specific increases were as follows: for LAMP2, sham vehicle = 1 ± 0.1, sham amlexanox = 1.104 ± 0.1, seizure vehicle = 0.557 ± 0.1, seizure amlexanox = 0.894 ± 0.1; for LC3B, sham vehicle = 1 ± 0.1, sham amlexanox = 1.051 ± 0.1, seizure vehicle = 0.451 ± 0.1, seizure amlexanox = 0.799 ± 0.1.

Furthermore, we measured the protein levels of inflammatory factors after seizures. The seizure vehicle group exhibited an overall increase in inflammatory factors, indicating heightened neuro-inflammation. However, in the amlexanox group, the levels of inflammatory factors were reduced compared to the seizure vehicle group. Notably, COX-2 decreased by 65.8% (Fig. 3 D, 3E). These findings demonstrate that amlexanox administration reduces neuro-inflammation and exerts a neuroprotective effect. The specific reductions were as follows: for COX-2, sham vehicle = 1 ± 0.2, sham amlexanox = 1.062 ± 0.1, seizure vehicle = 4.39 ± 1, seizure amlexanox = 1.501 ± 0.3.

In summary, administering amlexanox after a seizure was found to increase lysosomal function and autophagy, leading to a decrease in neuro-inflammatory factors. These results highlight the potential of amlexanox as a therapeutic agent for mitigating the adverse effects of seizures on neuronal health. The study contributes valuable insights into the neuroprotective properties of amlexanox, supporting its potential as a promising treatment for neurological disorders associated with seizures.

Amlexanox decreases neuronal death after pilocarpine-induced seizure

In our study, we used neural nuclei (NeuN) staining to evaluate the neuroprotective effects of amlexanox on neuron survival after inducing seizures with pilocarpine. At one week following the seizures, the animals were euthanized and their brain tissue was stained to analyze the hippocampal region.

The findings were significant: the amlexanox-treated group exhibited a substantial increase in the number of live neurons across all hippocampal sections compared to the seizure vehicle group (Fig. 4A, B - 4E). Notably, each hippocampal area showed a remarkable improvement. In the subiculum, there was a 59% increase in live neurons relative to the vehicle group. The cornu ammonis 1 (CA1) region displayed a 44.9% increase, cornu ammonis 3 (CA3) showed a 51% rise, and the dentate gyrus (DG) experienced a 51.3% increase. The specific statistics were as follows: in the subiculum, sham vehicle = 372 ± 35.4, sham amlexanox = 388 ± 16.7, seizure vehicle = 143 ± 14.9, seizure amlexanox = 330 ± 25.9; in CA1, sham vehicle = 441 ± 23, sham amlexanox = 485 ± 25.59, seizure vehicle = 152 ± 24.01, seizure amlexanox = 276 ± 24.64; in CA3, sham vehicle = 562 ± 17.28, sham amlexanox = 571 ± 20.31, seizure vehicle = 188 ± 25.88, seizure amlexanox = 383 ± 40.34; in the DG, sham vehicle = 97 ± 9.81, sham amlexanox = 95 ± 11.36, seizure vehicle = 29 ± 6.55, seizure amlexanox = 59 ± 11.64 (Fig. 4B–E). These increases were statistically significant, with $P < 0.05$. The results strongly support the neuroprotective role of amlexanox, underscoring its potential as a therapeutic agent for the reduction of neuronal damage and promotion of neuronal survival following seizures. The observed enhancement in the live neuron count across various regions of the hippocampus further emphasizes the beneficial impact of amlexanox on hippocampal functionality and cognitive processes.

Amlexanox mitigates glia cell activation following seizures

Following the induction of seizures, we conducted a thorough examination of glial cell activation, specifically targeting astrocytes and microglia. For the identification of activated glia cells, we utilized antibodies against glial fibrillary acidic protein (GFAP), complement 3(C3), ionized calcium-binding adapter molecule 1(Iba-1), and cluster of differentiation 68(CD68). C3 staining was used to detect activated

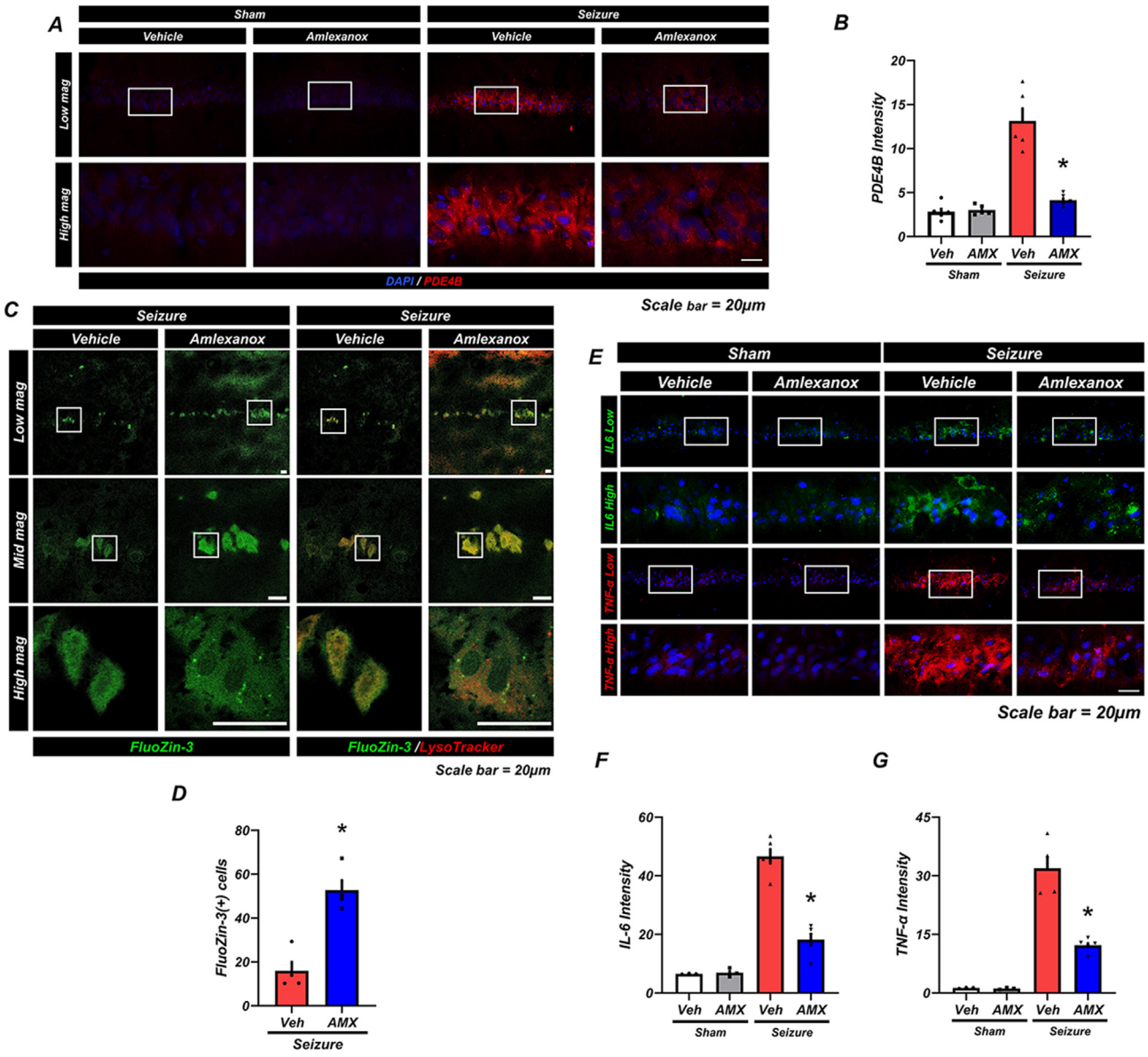

Fig. 2. Amlexanox's Effect on PDE4B Expression, Pro-Inflammatory Factors, and Zinc Levels in Lysosomes Following Seizures. A. PDE4B Staining: Illustrates phosphodiesterase-4B (PDE4B) expression (in red) 12 h after a seizure and in the sham groups. Neurons were visualized using DAPI, which was merged with PDE4B staining, highlighting the neuronal population. B. PDE4B Quantification Bar Graph: Compares the PDE4B levels between the vehicle and amlexanox groups following seizures. The analysis involved the sham vehicle (n = 5), sham amlexanox (n = 5), seizure vehicle (n = 5), and seizure amlexanox (n = 5) groups. The graph presents the mean ± S.E.M. data, showing a significant difference ($p < 0.05$) between the vehicle and amlexanox groups, as determined by the Bonferroni post hoc test following the Kruskal–Wallis test (chi-square = 13.834, df = 3, p = 0.003). C. Zinc Staining with FluoZin-3: Demonstrates staining with FluoZin-3 in the cornu ammonis 1 (CA1) area, performed 72 h after a seizure. LysoTracker was used in conjunction with FluoZin-3 staining. D. Zinc Quantification Bar Graph: Displays the comparison of the zinc levels in the vehicle and amlexanox groups following seizures, involving the seizure vehicle (n = 4) and seizure amlexanox (n = 4) groups. The graph shows the mean ± S.E.M. data, with a significant difference ($p < 0.05$) between the groups as per the Mann–Whitney *U* test (z = 2.309, p = 0.029). E-G. Inflammatory Factor Staining: Displays the interleukin-6 (IL-6, in green) and tumor necrosis factor-α (TNF-α, in red) staining conducted 12 h following seizures and in sham groups. DAPI was merged with IL-6 and TNF-α staining. Inflammatory Factor Quantification Bar Graph: Compares the levels of IL-6 and TNF-α between the vehicle and amlexanox groups following seizures. The analysis included the sham vehicle (n = 3), sham amlexanox (n = 3), seizure vehicle (n = 5), and seizure amlexanox (n = 5) groups. The data are the mean ± S.E.M., highlighting a significant difference ($p < 0.05$) between the groups as established by the Bonferroni post hoc test after the Kruskal–Wallis test (IL-6: chi-square = 13.412, df = 3, p = 0.004; TNF-α: chi-square = 13.412, df = 3, p = 0.004). Scale bar corresponds to 20 μm in all images in Fig. 2.

astrocytes of the A1 subtype, while CD68 staining helped us identify activated microglia of the M1 subtype. Our observations revealed a significant increase in glial cell activation following seizures. However, the administration of amlexanox effectively reduced the activation of glial cells (Fig. 5).

In the amlexanox-treated group, the number of activated astrocytes, as measured via the GFAP and C3 levels, showed a reduction of 68% compared to the seizure vehicle group (Fig. 5BandC). Additionally, the activated microglia levels, determined through the Iba-1 and CD68 markers, were reduced by 58.1% in the amlexanox group compared to the seizure vehicle group (Fig. 5EandF). These decreases were as follows: for GFAP, sham vehicle = 2.04 ± 0.49, sham amlexanox = 3.15 ± 0.48, seizure vehicle = 25.41 ± 2.58, seizure amlexanox = 9.65 ± 1.04; for C3, sham vehicle = 1.93 ± 0.46,

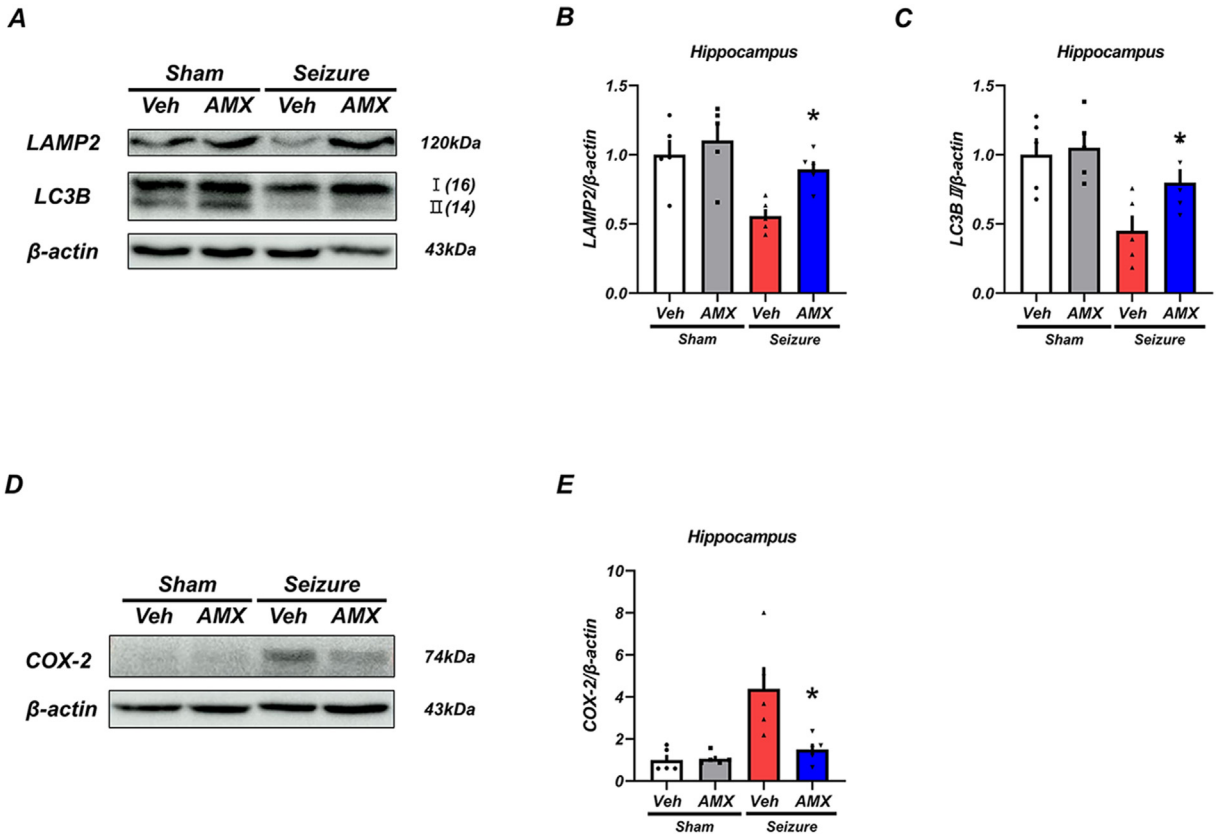

Fig. 3. Amlexanox Enhances Autophagy and Lysosomal Function While Reducing Neuroinflammation. A-C. LAMP2 and LC3B Expression Analysis via Western Blot: This segment illustrates the assessment of the lysosome-associated membrane protein 2 (LAMP2) and light chain 3B (LC3B) levels, indicators of lysosomal function and autophagy. The displayed results show the expression levels of LAMP2 and LC3B in various experimental samples. The accompanying bar graphs quantify these results, indicating the relative protein expression in comparison to the control group. A significant difference in protein levels was observed for both LAMP2 (Bonferroni post hoc test after Kruskal–Wallis test, chi-square = 10.063, df = 3, p = 0.018) and LC3B (Bonferroni post hoc test after Kruskal–Wallis test, chi-square = 10.406, df = 3, p = 0.015). D-E. COX-2 Expression Analysis via Western Blot: These sections cover the assessment of cyclooxygenase-2 (COX-2) expression, a marker for neuroinflammation. The results present the COX-2 expression levels in the experimental samples. The corresponding bar graph quantifies these results, showing the relative expression of COX-2 compared to the control group. The statistical analysis revealed a significant difference in COX-2 levels (Bonferroni post hoc test after Kruskal–Wallis test, chi-square = 11.709, df = 3, p = 0.008).

sham amlexanox = 1.71 ± 0.44, seizure vehicle = 17.98 ± 2.51, seizure amlexanox = 5.75 ± 1.07; for Iba-1, sham vehicle = 6.59 ± 1.31, sham amlexanox = 6.79 ± 1.29, seizure vehicle = 41.35 ± 4.5, seizure amlexanox = 16.22 ± 2.57; for CD68, sham vehicle = 1.64 ± 0.41, sham amlexanox = 1.68 ± 0.22, seizure vehicle = 18.42 ± 2.42, seizure amlexanox = 7.71 ± 1.31. Furthermore, the reduction in glial cell activation led to a corresponding decrease in neuroinflammatory factors, illustrating the beneficial impact of amlexanox on post-seizure inflammation.

In summary, the administration of amlexanox after seizures resulted in a substantial reduction in glial cell activation, particularly in activated astrocytes and microglia. This reduction in glial cell activation contributed to a notable decrease in neuro-inflammatory factors. These findings underscore the potential of amlexanox as a therapeutic agent for modulating glial cell activity and alleviating neuro-inflammatory responses following seizures. The study contributes valuable insights into the mechanisms of amlexanox's neuroprotective effects, which may hold significant implications for the treatment of neurological disorders associated with glial cell activation and inflammation.

Amlexanox alleviates oxidative stress and preserves microtubule integrity following seizures

Our study focused on evaluating the effects of amlexanox on oxidative stress and microtubule disruption following pilocarpine-induced seizures. We conducted brain section staining for 4-hydroxynonenal (4-HNE) to assess reactive oxygen species (ROS) and for microtubule-associated protein 2 (MAP2) to examine microtubule integrity. Our findings indicated a pronounced post-seizure increase in ROS levels in the hippocampus, with increases of 67.3% in the subiculum, 79.5% in CA1, 69.4% in CA3, and 67.4% in the DG compared to the sham vehicle group. However, amlexanox administration resulted in a substantial reduction in ROS levels: 57.4% in the subiculum, 67.6% in CA1, 59.9% in CA3, and 57.4% in the DG, as compared to the seizure vehicle group (Fig. 6F, G - 6J). The specific rates of decrease were as follows: in the subiculum, sham vehicle = 10.97 ± 0.83, sham amlexanox = 11.06 ± 0.99, seizure vehicle = 33.6 ± 4.06, seizure amlexanox = 14.32 ± 1.06; in CA1, sham vehicle = 7.76 ± 1.29, sham amlexanox = 6.29 ± 1.64, seizure vehicle = 37.91 ± 1.46, seizure amlexanox = 12.27 ± 1.64; in CA3, sham vehicle = 13.16 ± 1.14, sham amlexanox = 13.58 ± 0.84, seizure vehicle = 43.02 ± 3.58, seizure amlexanox = 17.24 ± 1.65; in the DG, sham vehicle = 12.22 ± 0.14, sham amlexanox = 11.32 ± 1.4, seizure vehicle = 37.46 ± 4.82, seizure amlexanox = 15.97 ± 1.2.

Additionally, the amlexanox treatment was associated with a significant improvement in microtubule integrity, as indicated by the increased MAP2 levels. The amlexanox group showed a marked increase in MAP2 levels in the subiculum, CA1, CA3, and DG compared to the seizure vehicle group, indicating enhanced microtubule stability (Fig. 6A, B - 6E). The specific rates of increase were as follows: in the subiculum, sham vehicle = 77.11 ± 1.29, sham amlexanox = 74.03 ±

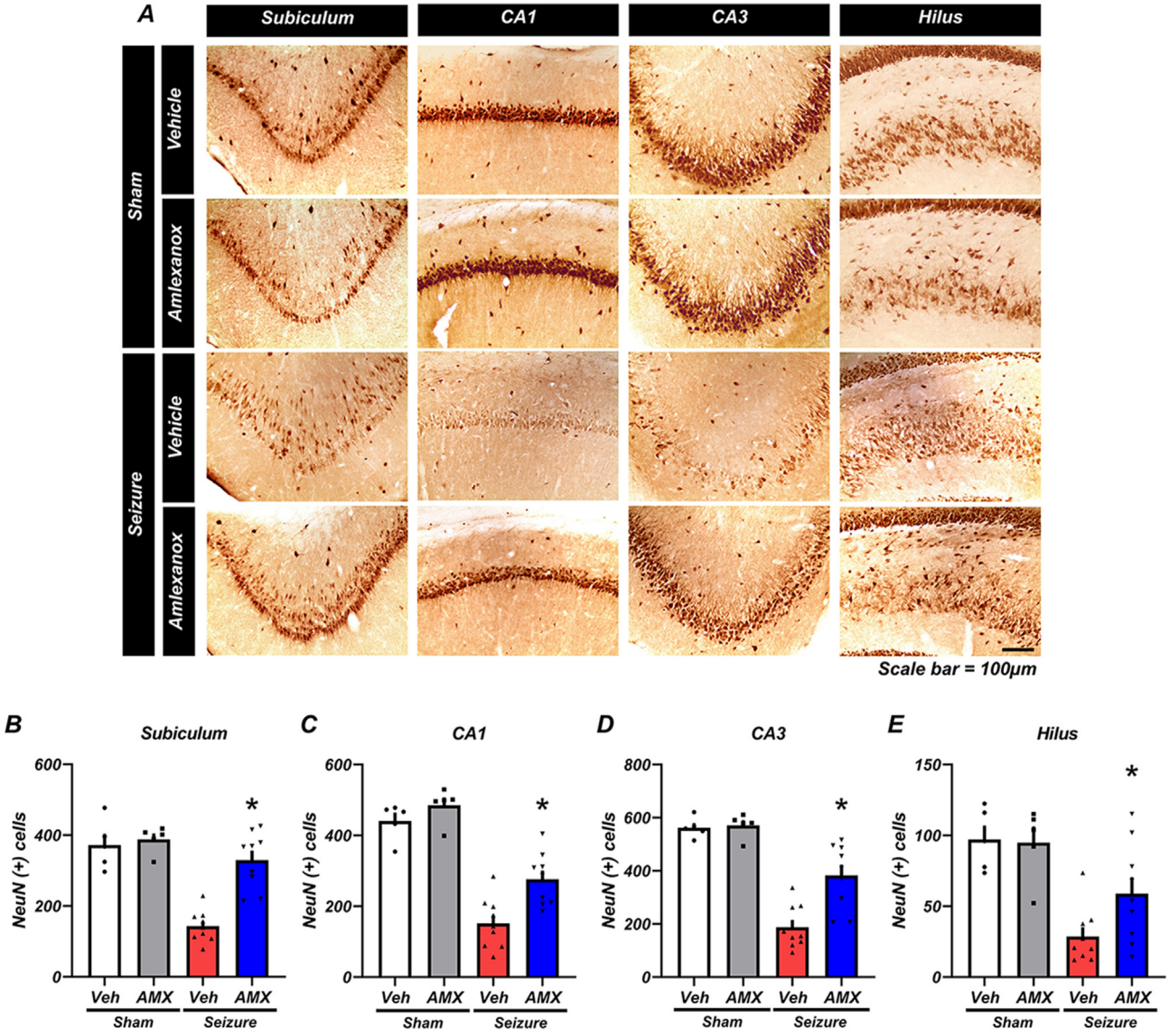

Fig. 4. Amlexanox Decreases Neuronal Death after Pilocarpine-Induced Seizures. A. NeuN Staining for Neuronal Survival: Depicts the use of neuronal nuclear protein (NeuN) staining to evaluate neuronal survival in the subiculum, CA1, cornu ammonis 3 (CA3), and hilus regions one week after pilocarpine-induced seizures, as well as in the sham group. The fluorescent images display the levels of NeuN-positive neurons in these specific brain regions. A scale bar indicating 100 μm is included, providing a reference for the size of the neuronal structures captured in the images. B-E. Quantitative Analysis of NeuN-Positive Neurons: These bar graphs compare the numbers of NeuN-positive neurons in different groups: sham vehicle (n = 5), sham amlexanox (n = 5), seizure vehicle group (n = 9), and seizure amlexanox (n = 9). Measurements were taken one week after seizures and in the sham group. Data are presented as the mean ± standard error of the mean (S.E.M.). The statistical analysis highlighted significant differences ($p < 0.05$) between the groups as follows: subiculum (Bonferroni post hoc test after Kruskal-Wallis test, chi-square = 18.067, df = 3, $p < 0.001$); CA1 (chi-square = 22.138, df = 3, $p < 0.001$); CA3 (chi-square = 21.476, df = 3, $p < 0.001$); hilus (chi-square = 15.005, df = 3, $p = 0.002$).

0.78, seizure vehicle = 31.42 ± 2.19, seizure amlexanox = 45.52 ± 1.98; in CA1, sham vehicle = 68.9 ± 1.6, sham amlexanox = 67.32 ± 0.85, seizure vehicle = 29.75 ± 2.39, seizure amlexanox = 45.74 ± 2.84; in CA3, sham vehicle = 73.59 ± 1.32, sham amlexanox = 70 ± 1.71, seizure vehicle = 43.08 ± 3.06, seizure amlexanox = 55.35 ± 1.62; in the DG, sham vehicle = 32.11 ± 2.37, sham amlexanox = 37.91 ± 1.79, seizure vehicle = 11.59 ± 0.98, seizure amlexanox = 29.64 ± 1.53. These observations suggest that increased ROS levels can lead to microtubule damage, contributing to neuronal death. However, amlexanox effectively reduces the ROS levels, thereby preventing microtubule damage and subsequent neuronal death. By mitigating oxidative stress, amlexanox helps to maintain the microtubules' integrity, which is vital in preserving neuronal function and preventing neurodegenerative processes.

These findings highlight the neuroprotective role of amlexanox in reducing oxidative stress and its adverse impacts on microtubule stability, thereby underscoring its therapeutic potential in managing seizures and associated neurological disorders.

Amlexanox mitigates Blood–Brain Barrier (BBB) disruption following seizures

In our study, we investigated the impact of amlexanox on blood-brain barrier (BBB) disruption following seizures by assessing the degree of IgG

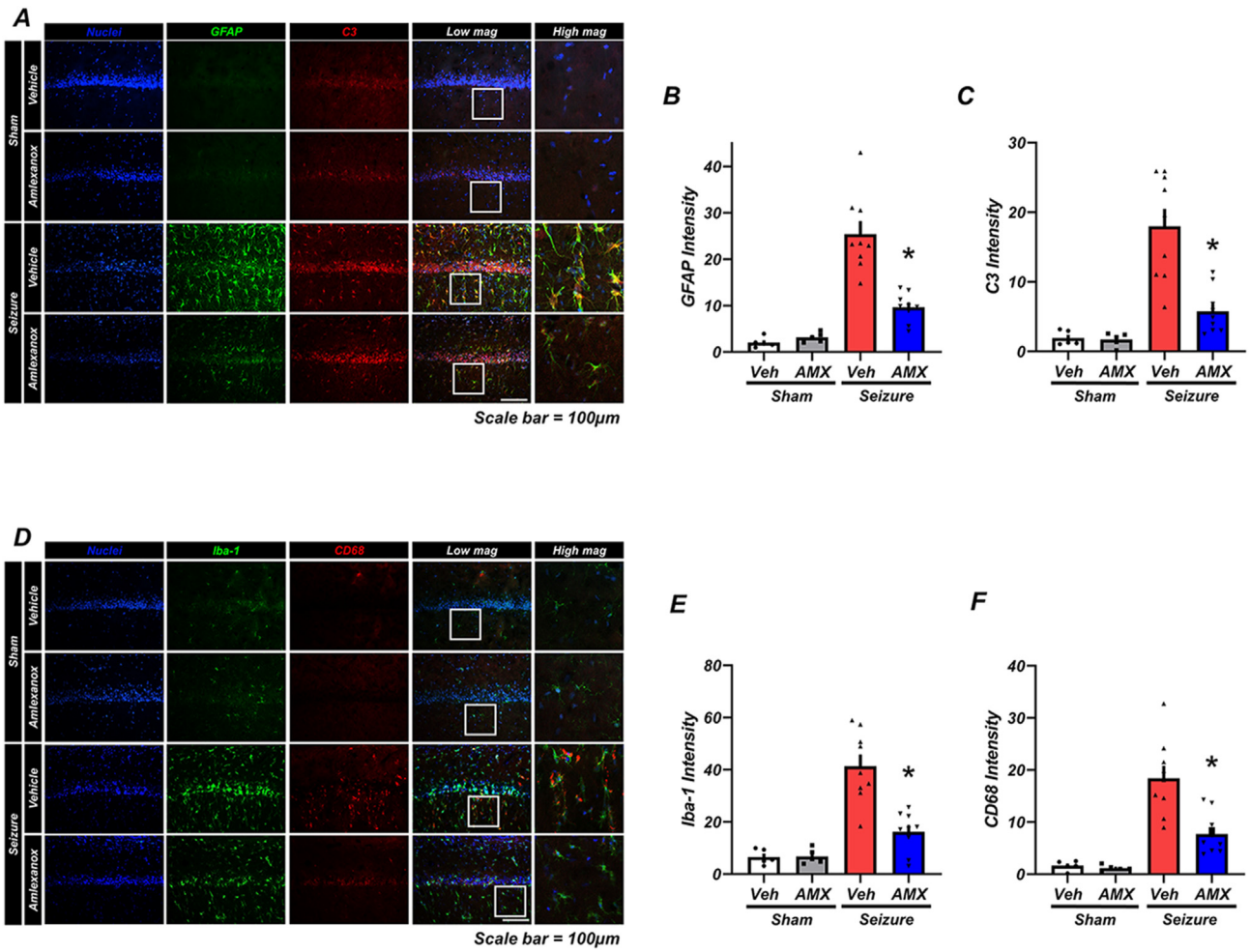

Fig. 5. Amlexanox Alleviates Glial Cell Activation Following Seizures. Panels A–C show staining for glial fibrillary acidic protein (GFAP, green) to highlight astrocytes in the CA1 region post-seizure and in the sham group. Complement 3 (C3, red) staining was used to identify activated astrocytes in both groups. The fluorescent images display the localization of GFAP, C3, and 4′,6-diamidino-2-phenylindole (DAPI, marking cell nuclei), accompanied by a scale bar of 100 μm. The accompanying bar graphs (B and C) illustrate the intensity of GFAP and C3 staining in the CA1 region. The statistical analysis revealed significant differences between the groups ($p < 0.05$), as shown by the Bonferroni post hoc test following a Kruskal–Wallis test (GFAP—chi-square = 24.108, degrees of freedom (df) = 3, $p < 0.001$; C3—chi-square = 21.375, df = 3, $p < 0.001$). Panels D–F feature staining for ionized calcium-binding adapter molecule 1 (Iba-1, green) to visualize microglia in the CA1 region post-seizure and in the sham group. Staining for cluster of differentiation 68 (CD68, red) was used to detect activated microglia. The images display Iba-1, CD68, and DAPI localization, with a scale bar of 100 μm. The bar graphs (E and F) present the intensity of the Iba-1 and CD68 staining in the CA1 area. The statistical analysis indicated significant differences between groups ($p < 0.05$), as confirmed by the Bonferroni post hoc test following the Kruskal–Wallis test (Iba-1—chi-square = 19.389, df = 3, $p < 0.001$; CD68—chi-square = 22.938, df = 3, $p < 0.001$).

leakage. Compared to the sham group, the seizure vehicle group exhibited a significant increase in IgG leakage, approximately 6.5 times higher. However, in the group treated with amlexanox, the degree of IgG leakage was reduced by half compared to the seizure vehicle group (Fig. 7A and B). The specific rates of decrease were as follows: sham vehicle = 1 ± 0.1, sham amlexanox = 1.15 ± 0.24, seizure vehicle = 6.89 ± 0.62, seizure amlexanox = 3.63 ± 0.58 (Fig. 7B). These results indicate that amlexanox administration significantly decreased the degree of IgG leakage compared to the seizure vehicle group. The findings strongly suggest that amlexanox treatment can effectively prevent BBB disruption following seizures.

Preserving the integrity of the BBB is vital for maintaining brain homeostasis and preventing the entry of harmful substances into the brain. The ability of amlexanox to reduce BBB permeability is noteworthy and may contribute to its neuroprotective effects. The observed reduction in IgG leakage indicates that amlexanox has the potential to safeguard the BBB and protect against the detrimental consequences of BBB disruption associated with seizures. This highlights amlexanox's promise as a therapeutic intervention for managing seizures and related neurological conditions.

Amlexanox enhances recovery of cognitive and neurological function following seizures

Our study provides substantial evidence that amlexanox enhances cognitive and neurological function following seizures. The research focused on three key areas: neuronal cell death, lysosomal and autophagic function in acute seizures, and behavioral assessments.

Firstly, to evaluate the impact of seizures on cognitive and neurological function, we employed two behavioral tests: the modified neurological severity score (mNSS) and the Barnes maze. The mNSS test, initiated 4 h following a seizure and extending over 2 weeks, revealed significant differences between the seizure amlexanox group and the seizure vehicle group, particularly on days 1 and 3–14 (Fig. 8 B). Additionally, the beam balance test, conducted at the end of the period, indicated notable improvements in behavioral recovery for the seizure

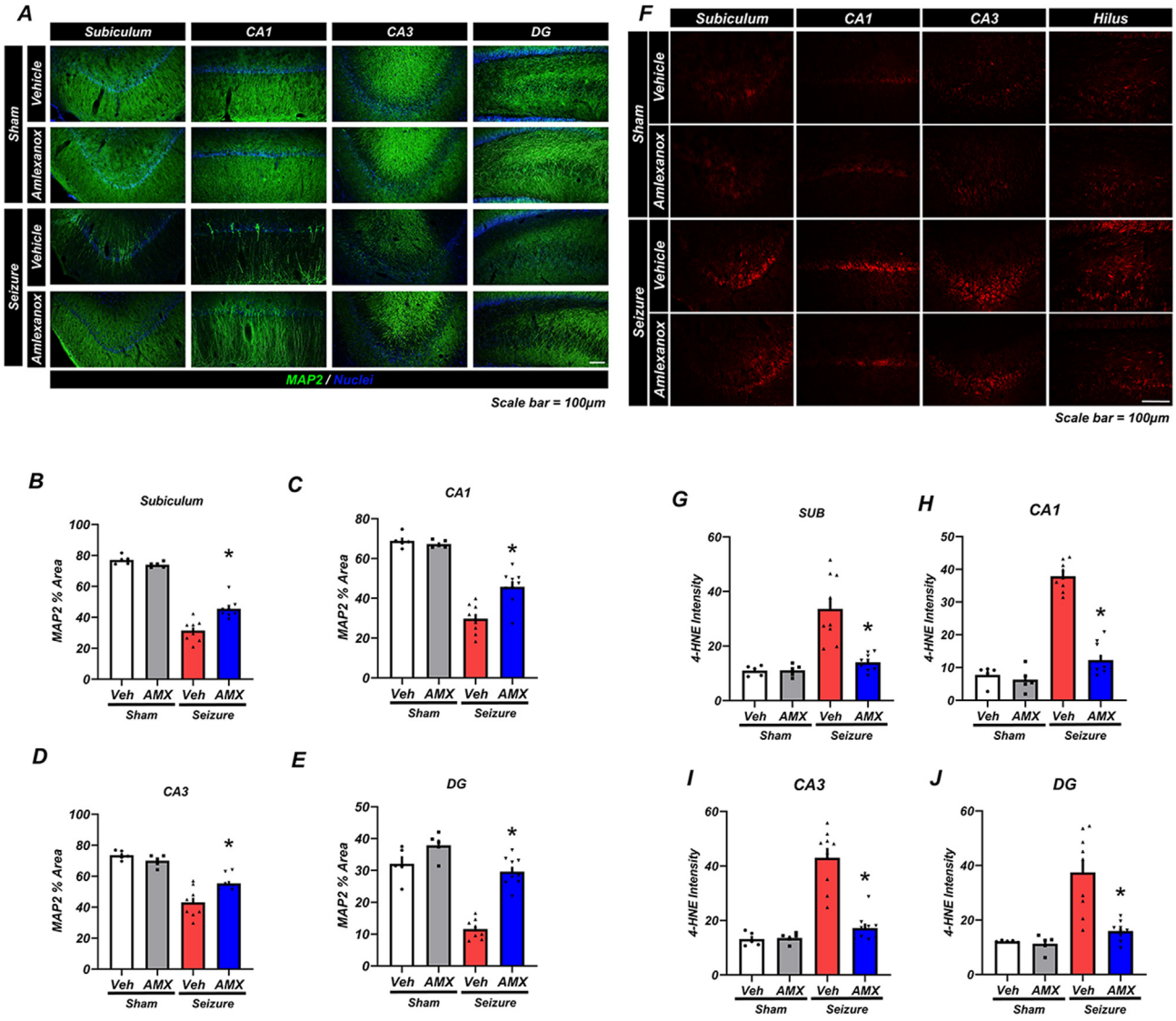

Fig. 6. Amlexanox Alleviates Oxidative Stress and Preserves Microtubule Integrity Following Seizures. A-E. Visualization of Microtubules with MAP2 Staining: Showcases microtubule-associated protein 2 (MAP2) staining (green fluorescence) across the hippocampus region, including the subiculum, CA1, CA3, and dentate gyrus (DG). The images display the distribution of MAP2 (green) alongside DAPI (blue), which indicates cell nuclei. A 100 μm scale bar provides a reference for the size of the structures. The bar graph depicts the percentage area of MAP2 staining in the entire hippocampus, including the sham vehicle (n = 5), sham amlexanox (n = 5), seizure vehicle (n = 9), and seizure amlexanox groups (n = 9). The statistical analysis, as shown by the Bonferroni post hoc test after the Kruskal–Wallis test, indicated significant differences between the groups in CA1 (chi-square = 22.32, df = 3, $p < 0.001$); data for other regions (subiculum—chi-square = 23.916, df = 3, $p < 0.001$, CA3—chi-square = 21.283, df = 3, $p < 0.001$, DG—chi-square = 20.817, df = 3, $p < 0.001$) are indicated as significant where relevant. F-J. ROS Detection Using 4-HNE Staining: Shows reactive oxygen species (ROS) levels assessed through 4-hydroxyl-2-nonenal (4-HNE) staining in the entire hippocampus, including the subiculum, CA1, CA3, and DG. The corresponding bar graph illustrates the intensity of 4-HNE staining across the hippocampus, including the sham vehicle (n = 5), sham amlexanox (n = 5), seizure vehicle (n = 9), and seizure amlexanox groups (n = 9). Mean values ± S.E.M. are shown. Statistical significance ($p < 0.05$) is highlighted between the groups (Bonferroni post hoc test after Kruskal–Wallis test: subiculum—chi-square = 19.342, df = 3, $p < 0.001$; CA1—chi-square = 20.563, df = 3, $p < 0.001$; CA3—chi-square = 19.078, df = 3, $p < 0.001$; DG—chi-square = 18.816, df = 3, $p < 0.001$).

amlexanox group (Videos 1–4). These findings underscore the severe neurological deficits caused by seizures, affecting motor, sensory, reflex, and balance capabilities. However, the post-seizure administration of amlexanox led to significant improvements in€ these neurological functions.

Supplementary video related to this article can be found at https://doi.org/10.1016/j.neurot.2024.e00357

Secondly, we conducted the Barnes maze test over a 2-week period following the mNSS test to assess cognitive function. In this setup, a disk with 20 holes was used, with only one hole leading to an escape. The experiment demonstrated that while the sham vehicle and sham amlexanox groups quickly located the escape hole, the seizure vehicle group struggled, often failing to find it or falling off the disk. In contrast, the seizure amlexanox group initially mirrored the seizure vehicle group's performance but gradually improved, showing significantly shorter escape times by days 2 and 4–14 (Fig. 8D).

Furthermore, the therapeutic effects of amlexanox in chronic seizure models were explored. NeuN staining, performed post-euthanasia on the seizure animal models, indicated a marked difference in the entire hippocampal region between the seizure vehicle and seizure amlexanox groups with chronic seizures, mirroring the findings for acute seizures (Fig. 8E, F - 8I). The observed rates of increase in the neuronal counts in various regions were as follows: 57.4% in the subiculum, 52.3% in CA1, 64.1% in CA3, and 54.7% in the DG. The specific statistics were as

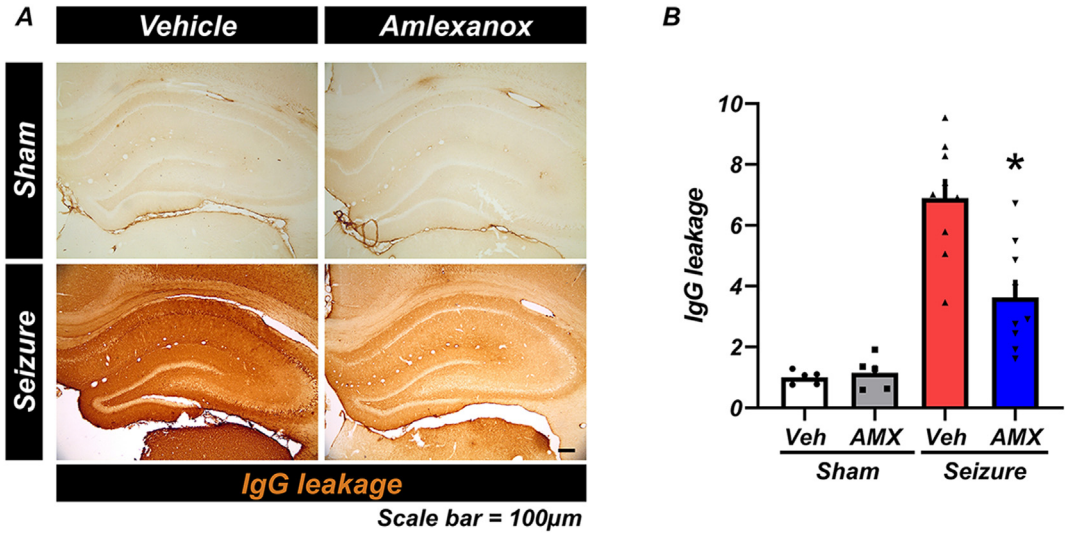

Fig. 7. Amlexanox Mitigates Blood–Brain Barrier Disruption Following Seizures. A. Hippocampal Immunostaining: Features micrographs of the hippocampus stained with anti-rat IgG to indicate blood–brain barrier (BBB) disruption. The scale bar represents a length of 100 μm, providing a reference for the size of the structures observed. B. IgG Leakage Quantification: The bar graph quantifies the extent of IgG leakage in the hippocampus, an indicator of BBB integrity. The dataset includes the sham vehicle (n = 5), sham amlexanox (n = 5), seizure vehicle (n = 9), and seizure amlexanox groups (n = 9), with values shown as the mean ± S.E.M. The statistical analysis confirmed the significant difference ($p < 0.05$) between the groups (Bonferroni post hoc test after Kruskal–Wallis test, chi-square = 22.029, df = 3, $p < 0.001$), demonstrating the effectiveness of amlexanox in reducing BBB disruption following seizures.

follows: in the subiculum, sham vehicle = 448 ± 5.31, sham amlexanox = 445 ± 9.89, seizure vehicle = 157 ± 21.85, seizure amlexanox = 369 ± 28.66; in CA1, sham vehicle = 464 ± 10.33, sham amlexanox = 485 ± 29.88, seizure vehicle = 108 ± 10.9, seizure amlexanox = 227 ± 37.02; in CA3, sham vehicle = 577 ± 11.92, sham amlexanox = 571 ± 15.34, seizure vehicle = 138 ± 38.91, seizure amlexanox = 384 ± 39.73; in the DG, sham vehicle = 116 ± 8.71, sham amlexanox = 111 ± 6.49, seizure vehicle = 26 ± 4.3, seizure amlexanox = 57 ± 13.58 (Fig. 8f–I). Detailed statistics for each region are provided, highlighting the significant differences across all measured parameters.

In conclusion, our results demonstrate that amlexanox is not only effective in acute seizure scenarios but also in chronic conditions. It facilitates gradual improvements in both neurological and cognitive function, underscoring its potential as a side-effect-free treatment with neuroprotective capabilities.

Discussion

The present study aimed to evaluate the therapeutic efficacy of amlexanox in pilocarpine-induced seizures and its potential neuroprotective effects. To achieve this, we conducted histological staining and Western blot analysis to confirm the therapeutic impact of amlexanox following seizures.

Our findings align with previous studies, indicating that pilocarpine-induced seizures lead to neuronal death, attributed to elevated levels of reactive oxygen species (ROS) and pro-inflammatory factors such as tumor necrosis factor α (TNF-α) [31–34]. Consistent with recent research, we explored the role of phosphodiesterase-4 (PDE4) overexpression in the development of neurological diseases [18,23]. Notably, inhibiting PDE4 has been shown to enhance lysosome function [24]. Based on these findings, we postulated that administering amlexanox, a non-selective PDE4 inhibitor, after seizures could enhance lysosome function, promote autophagy, and provide neuronal protection.

Our study specifically focused on PDE4B, as excessive expression of this subtype has been linked to neuronal death and various neurological disorders [22,35]. We investigated whether amlexanox, as a PDE4 inhibitor, could effectively suppress PDE4B expression. Our results demonstrated a decrease in PDE4B levels following seizures, indicating successful PDE4B inhibition with amlexanox treatment. These results are in line with the findings of Koh et al., who observed changes in intracellular zinc levels and alterations in lysosomal activity associated with PDE4B inhibition [24]. Our study indicates that targeting PDE4B with amlexanox may modulate cyclic adenosine monophosphate (cAMP) levels, regulate intracellular zinc, and impact lysosomal activity, potentially providing insights into the therapeutic potential of PDE4B inhibition in neurological disorders and related conditions.

Seizures are associated with oxidative stress, heightened glial cell activity, and the disruption of the blood–brain barrier (BBB). One of the key contributing factors is mitochondrial dysfunction, which leads to an increase in free radical production, ultimately resulting in neuronal death [36]. Our research indicates that the post-seizure administration of amlexanox can significantly mitigate the accumulation of intracellular free radicals and thereby prevent neuronal death. Furthermore, we explored the involvement of cyclooxygenase-2 (COX-2) in BBB disruption following seizures. This was achieved through a series of experiments, including a Western blot analysis and immunohistochemistry studies [37,38]. The results demonstrated a reduction in COX-2 expression and a corresponding decrease in BBB disruption in cases in which amlexanox was administered, suggesting its potential to exert neuroprotective effectsAstrocytes and microglia are essential glial cells in neuronal function [39]. Astrocytes play a crucial role in energy homeostasis and nutrient transport in neurons [40]. However, during seizures, astrocyte dysfunction can lead to the release of complement 3 (C3) when activated [41]. Similarly, M1 microglia become activated during seizures and release cluster of differentiation 68 (CD68) [42–44]. In our study, we confirmed glial cell activation during seizures and observed a decrease in glial cell activation following amlexanox administration. Additionally, excessive pro-inflammatory factors, including TNF-α and IL-6, are activated during seizures [14,45]. Our investigation of pro-inflammatory cytokines released by activated microglia, such as TNF-α and IL-6, demonstrated a decrease in their levels after amlexanox administration, suggesting a dampening of the inflammatory response.

Mitochondrial dysfunction leads to the generation of ROS due to an excessive influx of calcium ions (Ca^{2+}) [46]. Elevated levels of intracellular free radicals can lead to cell death, emphasizing the importance

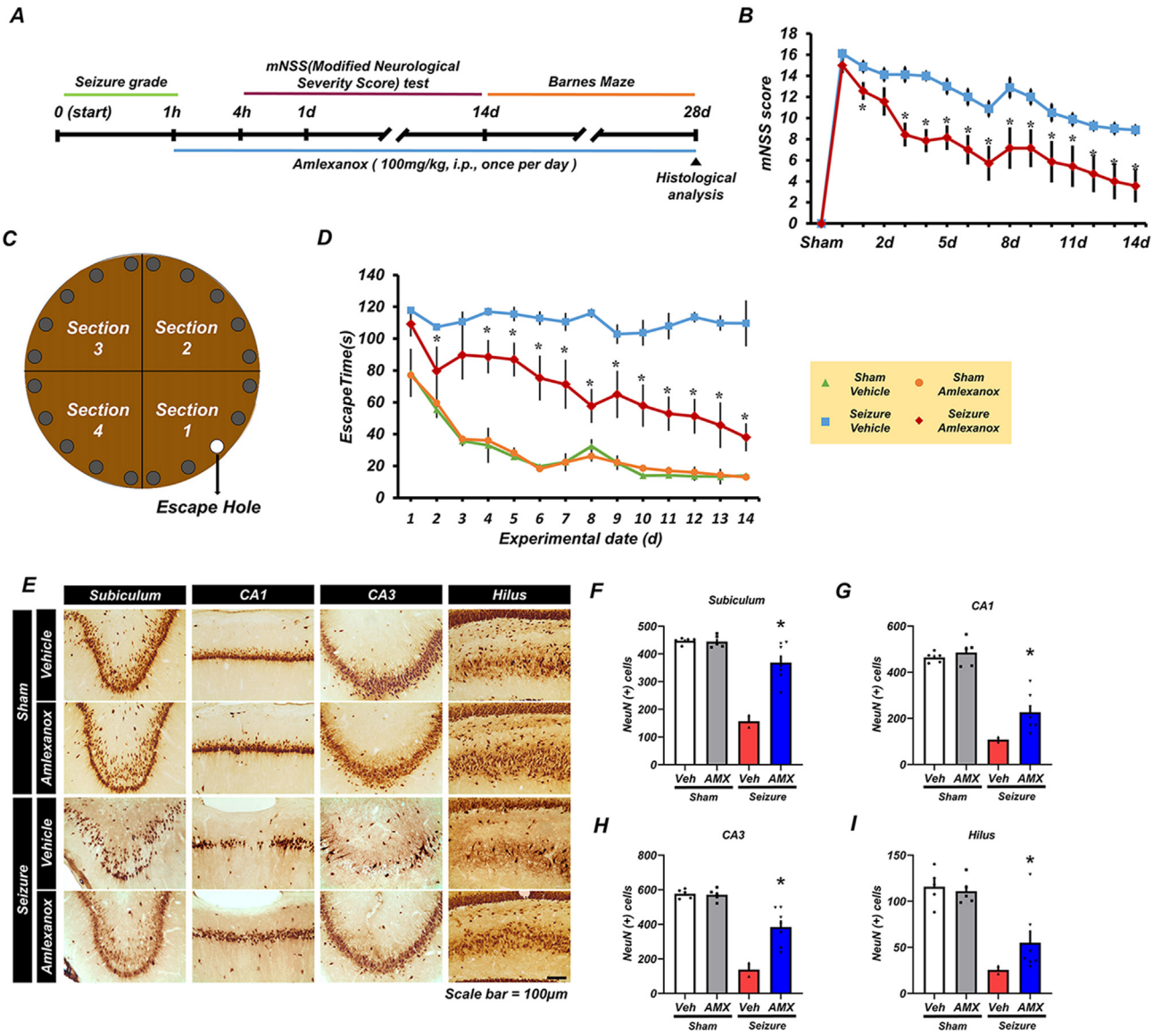

Fig. 8. Amlexanox's Effects on Cognitive and Neuological Function Following Seizures. A. Experimental Procedure: The study began with the modified neurological severity score (mNSS) test 4 h after seizure induction, continuing through day 14. From days 14–28, the Barnes maze test was conducted. Amlexanox was administered daily at a dose of 100 mg/kg via intraperitoneal injection until the end of the experiment. B. mNSS Scores: These were recorded from 4 h post-seizure to day 14, on a scale ranging from 0 to 18 points. Statistical significance was determined by ANOVA with repeated measures (mNSS: time: $F = 37.795$, $p < 0.001$; group: $F = 11.04$, $p = 0.004$; interaction: $F = 2.316$, $p = 0.005$). *$p < 0.05$. C. Barnes Maze Configuration: The maze consisted of a disk with a diameter of 122 cm, featuring an escape hole that was 7 cm in diameter. D. Barnes Maze Execution: Conducted from days 14–28 post-seizure with a time limit of 2 min (120s) per trial; failures were recorded as 120s. The statistical analysis involved ANOVA with repeated measures (Barnes maze: time: $F = 12.627$, $p < 0.001$; group: $F = 1.634$, $p = 0.016$; interaction: $F = 16.147$, $p < 0.001$). *$p < 0.05$. E. Neuronal Survival via NeuN Staining: Live neurons were stained with NeuN in the subiculum, CA1, CA3, and hilus areas one week after pilocarpine-induced seizures and in the sham group. Fluorescent images show NeuN-positive neurons with a 100 μm scale bar. F–I. Quantification of NeuN-Positive Neurons: The bar graphs compare the NeuN-positive neuron counts in the vehicle and amlexanox treatment groups post-seizure and in the sham group. The sample sizes include the sham vehicle (n = 5), sham amlexanox (n = 5), seizure vehicle (n = 2), and seizure amlexanox (n = 7) groups. Values are expressed as the mean ± S.E.M. Significance was assessed using the Bonferroni post hoc test following the Kruskal–Wallis test (subiculum: chi-square = 10.77, df = 3, $p = 0.013$; CA1: chi-square = 14.574, df = 3, $p = 0.002$; CA3: chi-square = 14.498, df = 3, $p = 0.002$; hilus: chi-square = 10.509, df = 3, $p = 0.015$). *$p < 0.05$.

of reducing reactive oxygen species (ROS) for cell survival. Our study observed a reduction in ROS levels in the amlexanox administration group, indicating that amlexanox decreases ROS through PDE4B inhibition following a seizure.

Lysosomes play a crucial role in the intracellular digestion of pathological or toxic waste materials [25,47]. Lysosomal function is enhanced by a decrease in lysosomal potential of hydrogen (pH), facilitated by zinc ions [25,48]. Autophagy, responsible for removing damaged organelles and waste materials [25,49], is facilitated by autolysosomes formed through the fusion of autophagosomes with lysosomes [50]. Our study confirmed a decrease in lysosomal function and autophagy following seizures, potentially contributing to neuronal cell death. In contrast, amlexanox administration increased the levels of lysosome-associated membrane protein 2 (LAMP2) and light chain 3B (LC3B), indicating enhanced lysosomal function and autophagy. Furthermore, our findings confirmed zinc accumulation in lysosomes after amlexanox treatment, leading to increased lysosomal pH and enhanced autophagy. These results indicate that amlexanox promotes autophagy and facilitates the efficient removal of toxic waste from neurons, ultimately improving lysosomal function and enhancing neuronal survival.

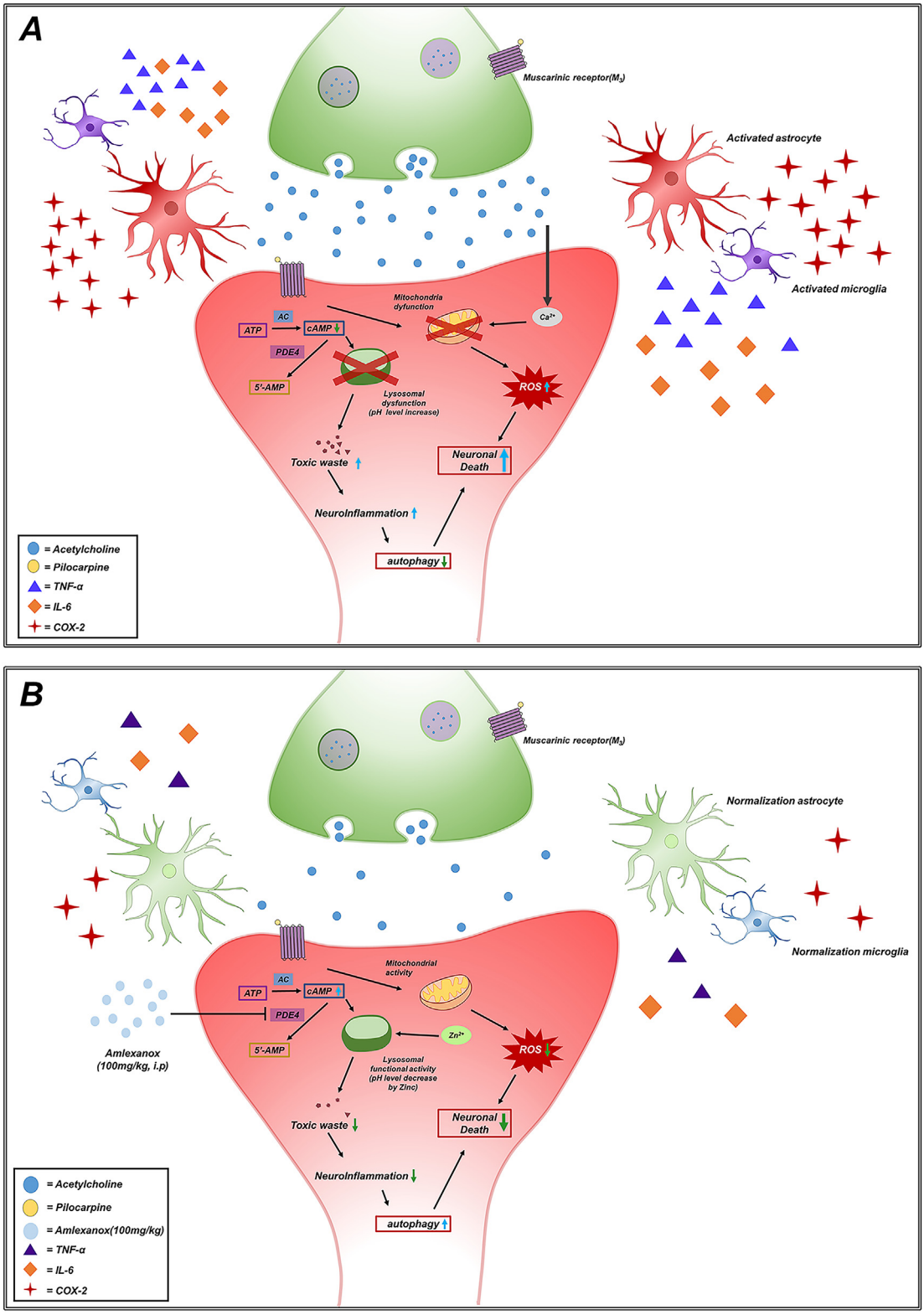

Fig. 9. Hypothetical Framework of the Current Study. A. Pilocarpine-Induced Seizure Schematic: This diagram provides a detailed representation of the process and critical stages in pilocarpine-induced seizures. It outlines the key steps and elements involved in the seizure induction mechanism. B. Amlexanox Administration Mechanism: This illustrates the role of amlexanox, a PDE4B inhibitor, highlighting its potential anti-inflammatory and neuroprotective effects following seizure occurrence. The diagram explains the conceptual mechanism of action of amlexanox in the context of seizure treatment and brain protection.

The protective role of amlexanox in acute epilepsy manifests through the prevention of neuronal death, which is primarily due to lysosomal dysfunction and increased autophagy. Previous research, including our own studies and those of others, has consistently reported significant declines in cognitive and neurological function following the onset of neurological diseases [34,51–53]. Notably, these studies did not focus on evaluating the seizure frequency and latency in a chronic epilepsy model. Therefore, our investigation was extended to consider the efficacy of

amlexanox in chronic epilepsy, specifically examining its impact on cognition and seizure frequencies. To validate our hypotheses, we employed the modified neurological severity score (mNSS) to assess neurological function and the Barnes maze for the cognitive evaluation. Furthermore, we analyzed the mortality rates to determine any potential adverse effects associated with long-term amlexanox treatment. After concluding these assessments, we performed neuronal nuclei (NeuN) staining to evaluate the neuronal loss. The findings indicated that prolonged treatment with amlexanox substantially enhanced the animals' neurological function and cognitive abilities, while also providing neuronal protection. However, it is important to note that the elevated mortality rate observed in the chronic phase of our model represents a limitation in this study.

In conclusion, our research elucidated the diverse neuroprotective effects of amlexanox in response to pilocarpine-induced seizures. This includes moderating glial cell activity, reducing the levels of pro-inflammatory cytokines, curbing free radical production, averting apoptosis, maintaining the integrity of the blood–brain barrier, and enhancing neurological and cognitive function. Our findings (as illustrated in Fig. 9) highlight amlexanox's potential as a therapeutic agent in the treatment of neurological disorders and similar conditions. This study makes a significant contribution to the field by providing insights that could guide the development of innovative neuroprotective strategies to manage seizure-related disorders. Nevertheless, additional research is necessary to fully understand the molecular mechanisms underlying amlexanox's effects and its broader clinical implications in neurological disease management.

Ethical approval

This study was approved by the Laboratory Animal Guides and Laboratory Rules published by the National Institute of Health (NIH), and this animal experiment was conducted according to the criteria of the Laboratory Animal Research Committee (protocol #Hallym 2022–22). The guidelines for this experiment were designed by ARRIVE (Animal Research: Reporting in Vivo Experiment).

Authors contributions

Conceptualization: S.W.S., J.K.P. and H.W.Y. Methodology: H.W.Y. Validation: H.W.Y. Formal Analysis: H.W.Y. Investigation: H.W.Y., A.R.K., S.H.L., B.S.K., M.K.P., C.J.L., S.Y.W., S.W.P., D.Y.K., H.H.J., B.Y.C., and W.I.Y. Data Curation: H.W.Y. Writing - Original Draft Preparation: H.W.Y. Writing - Review and Editing: J.K.P., S.H.L., A.R.K., and S.W.S. Visualization: B.S.K., M.K.P., and H.W.Y. Supervision: H.C.C., H.K.S., and S.W.S. All authors have read the journal's authorship agreement. The manuscript has been reviewed and approved by all authors.

Funding

This research was supported by a grant of the Korea Dementia Research Project through the Korea Dementia Research Center (KDRC), funded by the Ministry of Health & Welfare and Ministry of Science and ICT, Republic of Korea (grant number: HU20C0206), which was awarded to S.W.S. Additionally, this work was supported by the Hallym University Research Fund (MHC-202402-003), and by the National Research Foundation (NRF) (No. RS-2023-00214437), which was awarded to J.K.P.

Availability of data and materials

N/A.

Declaration of competing interest

The authors declare that they have no known competing financial interests or personal relationships that could have appeared to influence the work reported in this paper.

Appendix A. Supplementary data

Supplementary data to this article can be found online at https://doi.org/10.1016/j.neurot.2024.e00357.

References

[1] Beghi E, Giussani G, Sander JW. The natural history and prognosis of epilepsy. Epileptic Disord 2015;17(3):243–53.
[2] Pascual MR. Temporal lobe epilepsy: clinical semiology and neurophysiological studies. Semin Ultrasound CT MR 2007;28(6):416–23.
[3] Dingledine R, Varvel NH, Dudek FE. When and how do seizures kill neurons, and is cell death relevant to epileptogenesis? Adv Exp Med Biol 2014;813:109–22.
[4] Kapur J, Stringer JL, Lothman EW. Evidence that repetitive seizures in the hippocampus cause a lasting reduction of GABAergic inhibition. J Neurophysiol 1989;61(2):417–26.
[5] Manford M. Recent advances in epilepsy. J Neurol 2017;264(8):1811–24.
[6] Naylor DE, Liu H, Niquet J, Wasterlain CG. Rapid surface accumulation of NMDA receptors increases glutamatergic excitation during status epilepticus. Neurobiol Dis 2013;54:225–38.
[7] Guo C, Ma YY. Calcium permeable-AMPA receptors and excitotoxicity in neurological disorders. Front Neural Circ 2021;15:711564.
[8] Goldberg EM, Coulter DA. Mechanisms of epileptogenesis: a convergence on neural circuit dysfunction. Nat Rev Neurosci 2013;14(5):337–49.
[9] Xiang T, Luo X, Ye L, Huang H, Wu Y. Klotho alleviates NLRP3 inflammasome-mediated neuroinflammation in a temporal lobe epilepsy rat model by activating the Nrf2 signaling pathway. Epilepsy Behav 2022;128:108509.
[10] Laxer KD, Trinka E, Hirsch LJ, Cendes F, Langfitt J, Delanty N, et al. The consequences of refractory epilepsy and its treatment. Epilepsy Behav 2014;37:59–70.
[11] Lull ME, Block ML. Microglial activation and chronic neurodegeneration. Neurotherapeutics 2010;7(4):354–65.
[12] Dong H, Cui B, Hao X. MicroRNA-22 alleviates inflammation in ischemic stroke via p38 MAPK pathways. Mol Med Rep 2019;20(1):735–44.
[13] Wei P, Wang K, Luo C, Huang Y, Misilimu D, Wen H, et al. Cordycepin confers long-term neuroprotection via inhibiting neutrophil infiltration and neuroinflammation after traumatic brain injury. J Neuroinflammation 2021;18(1):137.
[14] Joseph SA, Lynd-Balta E, O'Banion MK, Rappold PM, Daschner J, Allen A, et al. Enhanced cyclooxygenase-2 expression in olfactory-limbic forebrain following kainate-induced seizures. Neuroscience 2006;140(3):1051–65.
[15] Serrano GE, Lelutiu N, Rojas A, Cochi S, Shaw R, Makinson CD, et al. Ablation of cyclooxygenase-2 in forebrain neurons is neuroprotective and dampens brain inflammation after status epilepticus. J Neurosci 2011;31(42):14850–60.
[16] Rawat C, Kukal S, Dahiya UR, Kukreti R. Cyclooxygenase-2 (COX-2) inhibitors: future therapeutic strategies for epilepsy management. J Neuroinflammation 2019;16(1):197.
[17] Pellacani C, Costa LG. Role of autophagy in environmental neurotoxicity. Environ Pollut 2018;235:791–805.
[18] Wang H, Gaur U, Xiao J, Xu B, Xu J, Zheng W. Targeting phosphodiesterase 4 as a potential therapeutic strategy for enhancing neuroplasticity following ischemic stroke. Int J Biol Sci 2018;14(12):1745–54.
[19] Zhang H, Kong Q, Wang J, Jiang Y, Hua H. Complex roles of cAMP-PKA-CREB signaling in cancer. Exp Hematol Oncol 2020;9(1):32.
[20] Rombaut B, Kessels S, Schepers M, Tiane A, Paes D, Solomina Y, et al. PDE inhibition in distinct cell types to reclaim the balance of synaptic plasticity. Theranostics 2021;11(5):2080–97.
[21] Bhat A, Ray B, Mahalakshmi AM, Tuladhar S, Nandakumar DN, Srinivasan M, et al. Phosphodiesterase-4 enzyme as a therapeutic target in neurological disorders. Pharmacol Res 2020;160:105078.
[22] Gretarsdottir S, Thorleifsson G, Reynisdottir ST, Manolescu A, Jonsdottir S, Jonsdottir T, et al. The gene encoding phosphodiesterase 4D confers risk of ischemic stroke. Nat Genet 2003;35(2):131–8.
[23] Essam RM, Kandil EA. p-CREB and p-DARPP-32 orchestrating the modulatory role of cAMP/PKA signaling pathway enhanced by Roflumilast in rotenone-induced Parkinson's disease in rats. Chem Biol Interact 2023;372:110366.
[24] Koh JY, Kim HN, Hwang JJ, Kim YH, Park SE. Lysosomal dysfunction in proteinopathic neurodegenerative disorders: possible therapeutic roles of cAMP and zinc. Mol Brain 2019;12(1):18.
[25] Kim KR, Park SE, Hong JY, Koh JY, Cho DH, Hwang JJ, et al. Zinc enhances autophagic flux and lysosomal function through transcription factor EB activation and V-ATPase assembly. Front Cell Neurosci 2022;16:895750.

[26] Dosanjh A, Won CY. Amlexanox: a novel therapeutic for atopic, metabolic, and inflammatory disease. Yale J Biol Med 2020;93(5):759–63.
[27] Han Y, Hou R, Zhang X, Liu H, Gao Y, Li X, et al. Amlexanox exerts anti-inflammatory actions by targeting phosphodiesterase 4B in lipopolysaccharide-activated macrophages. Biochim Biophys Acta Mol Cell Res 2020;1867(10): 118766.
[28] He Q, Xia X, Yao K, Zeng J, Wang W, Wu Q, et al. Amlexanox reversed non-alcoholic fatty liver disease through IKKepsilon inhibition of hepatic stellate cell. Life Sci 2019;239:117010.
[29] Reilly SM, Chiang SH, Decker SJ, Chang L, Uhm M, Larsen MJ, et al. An inhibitor of the protein kinases TBK1 and IKK-varepsilon improves obesity-related metabolic dysfunctions in mice. Nat Med 2013;19(3):313–21.
[30] Oral EA, Reilly SM, Gomez AV, Meral R, Butz L, Ajluni N, et al. Inhibition of IKKvarepsilon and TBK1 improves glucose control in a subset of patients with type 2 diabetes. Cell Metabol 2017;26(1):157–170 e7.
[31] Lee SH, Choi BY, Kho AR, Jeong JH, Hong DK, Lee SH, et al. Protective effects of protocatechuic acid on seizure-induced neuronal death. Int J Mol Sci 2018; 19(1).
[32] Kang DH, Choi BY, Lee SH, Kho AR, Jeong JH, Hong DK, et al. Effects of cerebrolysin on hippocampal neuronal death after pilocarpine-induced seizure. Front Neurosci 2020;14:568813.
[33] Jeong JH, Lee SH, Kho AR, Hong DK, Kang DH, Kang BS, et al. The transient receptor potential melastatin 7 (TRPM7) inhibitors suppress seizure-induced neuron death by inhibiting zinc neurotoxicity. Int J Mol Sci 2020;21(21).
[34] Lee SH, Choi BY, Kho AR, Hong DK, Kang BS, Park MK, et al. Combined treatment of dichloroacetic acid and pyruvate increased neuronal survival after seizure. Nutrients 2022;14(22).
[35] Li YF, Cheng YF, Huang Y, Conti M, Wilson SP, O'Donnell JM, et al. Phosphodiesterase-4D knock-out and RNA interference-mediated knock-down enhance memory and increase hippocampal neurogenesis via increased cAMP signaling. J Neurosci 2011;31(1):172–83.
[36] Lin MT, Beal MF. Mitochondrial dysfunction and oxidative stress in neurodegenerative diseases. Nature 2006;443(7113):787–95.
[37] Lee B, Dziema H, Lee KH, Choi YS, Obrietan K. CRE-mediated transcription and COX-2 expression in the pilocarpine model of status epilepticus. Neurobiol Dis 2007;25(1):80–91.
[38] Rawat C, Kutum R, Kukal S, Srivastava A, Dahiya UR, Kushwaha S, et al. Downregulation of peripheral PTGS2/COX-2 in response to valproate treatment in patients with epilepsy. Sci Rep 2020;10(1):2546.
[39] Norden DM, Trojanowski PJ, Villanueva E, Navarro E, Godbout JP. Sequential activation of microglia and astrocyte cytokine expression precedes increased Iba-1 or GFAP immunoreactivity following systemic immune challenge. Glia 2016;64(2): 300–16.
[40] Boison D, Steinhauser C. Epilepsy and astrocyte energy metabolism. Glia 2018; 66(6):1235–43.
[41] Wei Y, Chen T, Bosco DB, Xie M, Zheng J, Dheer A, et al. The complement C3-C3aR pathway mediates microglia-astrocyte interaction following status epilepticus. Glia 2021;69(5):1155–69.
[42] Yuan L, Neufeld AH. Activated microglia in the human glaucomatous optic nerve head. J Neurosci Res 2001;64(5):523–32.
[43] Benson MJ, Manzanero S, Borges K. Complex alterations in microglial M1/M2 markers during the development of epilepsy in two mouse models. Epilepsia 2015; 56(6):895–905.
[44] Alam Y, Mugge LA, Purdy J, Mrak RE, Schroeder J. Long-term seizure disorder caused by a dermoid cyst with catastrophic developments. Cureus 2018;10(9): e3272.
[45] Rana A, Musto AE. The role of inflammation in the development of epilepsy. J Neuroinflammation 2018;15(1):144.
[46] Kawamata H, Manfredi G. Mitochondrial dysfunction and intracellular calcium dysregulation in ALS. Mech Ageing Dev 2010;131(7-8):517–26.
[47] Saftig P, Haas A. Turn up the lysosome. Nat Cell Biol 2016;18(10):1025–7.
[48] Zeng J, Shirihai OS, Grinstaff MW. Modulating lysosomal pH: a molecular and nanoscale materials design perspective. J Life Sci 2020;2(4):25–37.
[49] Glick D, Barth S, Macleod KF. Autophagy: cellular and molecular mechanisms. J Pathol 2010;221(1):3–12.
[50] Galluzzi L, Green DR. Autophagy-independent functions of the autophagy machinery. Cell 2019;177(7):1682–99.
[51] Lee SH, Choi BY, Kim JH, Kho AR, Sohn M, Song HK, et al. Late treatment with choline alfoscerate (l-alpha glycerylphosphorylcholine, alpha-GPC) increases hippocampal neurogenesis and provides protection against seizure-induced neuronal death and cognitive impairment. Brain Res 2017;1654(Pt A):66–76.
[52] Hong DK, Eom JW, Kho AR, Lee SH, Kang BS, Lee SH, et al. The inhibition of zinc excitotoxicity and AMPK phosphorylation by a novel zinc chelator, 2G11, ameliorates neuronal death induced by global cerebral ischemia. Antioxidants 2022;11(11).
[53] Dyomina AV, Smolensky IV, Zaitsev AV. Refinement of the Barnes and Morris water maze protocols improves characterization of spatial cognitive deficits in the lithium-pilocarpine rat model of epilepsy. Epilepsy Behav 2023;147:109391.